

## Phases of cytoplasmic and cortical reorganizations of the ascidian zygote between fertilization and first division

Fabrice Roegiers\*, Chakib Djediat, Rémi Dumollard, Christian Rouvière and Christian Sardet‡

Bio Mar Cell, Unité de Biologie du Développement – UMR 643, CNRS/UPMC, Station Zoologique, Villefranche-sur-mer, 06230, France

\*Present address: Howard Hughes Medical Institute, Room U226, UCSF Box 0725, 533 Parnassus Avenue, San Francisco, CA 94143-0725, USA

‡Author for correspondence (e-mail: sardet@ccrv.obs-vlfr.fr)

Accepted 27 April; published on WWW 21 June 1999

### SUMMARY

Many eggs undergo reorganizations that localize determinants specifying the developmental axes and the differentiation of various cell types. In ascidians, fertilization triggers spectacular reorganizations that result in the formation and localization of distinct cytoplasmic domains that are inherited by early blastomeres that develop autonomously.

By applying various imaging techniques to the transparent eggs of *Phallusia mammillata*, we now define 9 events and phases in the reorganization of the surface, cortex and the cytoplasm between fertilization and first cleavage. We show that two of the domains that preexist in the egg (the ER-rich cortical domain and the mitochondria-rich subcortical myoplasm) are localized successively by a microfilament-driven cortical contraction, a microtubule-driven migration and rotation of the sperm aster with respect to the cortex, and finally, a novel microfilament-dependant relaxation of the vegetal cortex. The phases of reorganization we have observed can best be explained in terms of cell cycle-regulated phases of coupling, uncoupling

and recoupling of the motions of cortical and subcortical layers (ER-rich cortical domain and mitochondria-rich domain) with respect to the surface of the zygote. At the end of the meiotic cell cycle we can distinguish up to 5 cortical and cytoplasmic domains (including two novel ones; the vegetal body and a yolk-rich domain) layered against the vegetal cortex. We have also analyzed how the myoplasm is partitioned into distinct blastomeres at the 32-cell stage and the effects on development of the ablation of precisely located small fragments.

On the basis of our observations and of the ablation/transplantation experiments done in the zygotes of *Phallusia* and several other ascidians, we suggest that the determinants for unequal cleavage, gastrulation and for the differentiation of muscle and endoderm cells may reside in 4 distinct cortical and cytoplasmic domains localized in the egg between fertilization and cleavage.

Key words: Ascidian, Egg, Zygote, Fertilization, Development, Cytoplasmic reorganization, Cytoplasmic domain, Cortex

### INTRODUCTION

Ascidians are marine invertebrates (urochordates/tunicates) that develop rapidly into simple tadpoles made of half a dozen types of tissues and less than 3000 cells (Satoh, 1994). Due to their well defined cell lineages and the fact that important developmental events are under the control of a small set of genes shared by vertebrates and invertebrates, ascidian eggs and embryos are gaining popularity for use in developmental studies (Satoh et al., 1996; DiGregorio and Levine, 1998). Early in this century, Conklin observed that eggs and zygotes of the ascidian *Styela* were composed of various cytoplasmic regions or plasms (ooplasm, protoplasm, mesoplasm) that were formed and/or localized in different regions of the zygote. He called the process cytoplasmic localization (which later came to be known as 'ooplasmic segregation'). Conklin observed that some of the colored plasms formed during oogenesis relocated between fertilization and first cleavage. In subsequent cleavages these and newly appearing plasms were

partitioned into different blastomeres and seemed to associate with particular cell fates (Conklin, 1905b). One such plasm (the yellow protoplasm or mesoplasm of *Styela*), is a mitochondria-rich region of the egg formed during oogenesis that is an essential part of a cytoplasmic domain known as the myoplasm (Conklin, 1905a; Jeffery and Swalla, 1990; Jeffery, 1995). The bulk of the myoplasm is localized in the posterior region of the zygote and is inherited principally by the blastomeres that differentiate into the primary muscle cells of the ascidian tadpole. The ablation of blastomeres or fragments of the zygote with large amounts of myoplasm is sufficient to abolish the differentiation of primary muscle cells (Meedel et al., 1987; Nishida, 1992). Other ablation experiments show that specific regions of the zygote contain the potential for unequal cleavage division, gastrulation or the formation of ectodermal and endodermal tissues (Bates and Jeffery, 1987; Nishida, 1993, 1994, 1996). Furthermore, if ablated cytoplasmic or cortical fragments are transplanted ectopically, the structures and tissues normally expressed in the ablated region appear at

the ectopic site (reviewed by Nishida, 1997). In such experiments one presumably deletes or transfers determinants and/or functional structures residing in different cortical and cytoplasmic domains.

The relocalizations in the ascidian zygote are thought to occur in two major phases (reviewed by Sawada, 1988; Jeffery and Bates, 1989; Sardet et al., 1994; Fernandez et al., 1998). First, the fertilizing sperm triggers a cortical contraction that travels across the egg in the animal-vegetal direction (Speksnijder et al., 1990a; Roegiers et al., 1995). As a result, in *Phallusia mammillata*, 3 domains, a microvilli-rich surface domain, a cortical endoplasmic reticulum (ER)-rich domain and the subcortical mitochondria-rich domain (myoplasm), are concentrated in and around a transient structure called the contraction pole, which forms in the vegetal pole region (Gualtieri and Sardet, 1989; Sardet et al., 1989; Speksnijder et al., 1993; Roegiers et al., 1995). This first phase is followed by a second major phase of cytoplasmic and cortical reorganization after completion of the meiotic cell cycle. During this second phase, the bulk of the myoplasm and vegetal cortical ER domain translocate along the posterior cortex towards the center of the sperm aster and the pronuclei. The aster, pronuclei and adjoining myoplasm and ER domains then migrate to the center of the egg (Sawada and Schatten, 1988; Sardet et al., 1989; Sawada and Schatten, 1989; Speksnijder et al., 1993). These successive phases of relocalization position the bulk of the myoplasm and ER-rich cortical domains towards the future posterior pole of the embryo.

This seems, however, a simplistic view of the reorganizations. In previous work we had already noted that the second major phase of relocalization consisted of 2 subphases. In addition subtler events occurred such as the periodic contractions and relaxations of the egg undergoing completion of meiosis and the transient formation of a vegetal protrusion, 'the vegetal button' before the onset of the second phase of reorganization (Sardet et al., 1989; Roegiers et al., 1995). We have now re-examined these events and their significance. We were also interested in defining the various domains formed in the zygote, the forces involved in their translocations and whether their movements were coupled. While it was clear that the 3 surface, cortical and subcortical domains previously identified in *Phallusia* moved vegetally in a coordinated fashion during the initial cortical contraction it appeared that later, the cortical ER domain and subcortical myoplasm moved posteriorly independently of any surface movements (Sardet et al., 1989; Speksnijder et al., 1993).

We have now carried out a full analysis of cytoplasmic, cortical and surface reorganizations in the clear egg of *Phallusia mammillata* using imaging of organelles and cytoskeletal elements, studying surface motions and using microfilament and microtubule inhibitors. As a result of this analysis we can define 9 events and phases (including the major phases discussed above and a novel phase) that participate in the formation and localization of the different domains. We show that 5 surface, cortical and cytoplasmic domains can be defined in the vegetal pole region of the zygote at the end of the meiotic cell cycle. We have also started to examine the importance of these domains by removing precisely located small fragments at the periphery of the zygote.

Our results provide a revised framework for the analysis of the role of cytoplasmic and cortical reorganizations in development of the ascidian embryo and for the interpretation of ablation/transplantation experiments in the ascidian zygote.

## MATERIALS AND METHODS

### Biological material

The tunicate *Phallusia mammillata* (Ascidiae, Tunicata) was collected and its gametes handled as described previously (Zalokar and Sardet, 1984; Sardet et al., 1989; Speksnijder et al., 1989b; Sardet et al., 1992). Eggs were dechorionated, fertilized, cultured and fixed as reported in these publications.

### Vital labelling and marking of eggs and embryos

For observations of the myoplasm, mitochondria were stained with the carbocyanine dye DiOC<sub>2</sub>(3) or Mitotracker (Molecular Probes, Eugene, Oregon) for 15–20 minutes (0.5 µg/ml DiOC<sub>2</sub>(3) or 1 µM Mitotracker in sea water buffered with TAPS (N-tris[hydroxymethyl]methyl-3-aminopropane sulfonic acid) (TAPS SW), pH 8.3 either before or after fertilization (Sardet et al., 1989). For observations of the endoplasmic reticulum, a small oil droplet saturated with DiIc<sub>16</sub> was injected into unfertilized eggs (Speksnijder et al., 1993). In order to study surface dynamics, unfertilized eggs were incubated with a suspension of washed 1 µm FITC fluospheres (Molecular Probes; 0.08% v/v washed in TAPS SW) for 30 minutes prior to fertilization. Alternatively, Nile blue particles were attached to the eggs as described by Roegiers et al. (1995).

To observe microtubule dynamics, unfertilized eggs were microinjected with Rhodamine-labelled pig brain tubulin prepared as described previously (Houliston et al., 1993). Microinjected eggs were allowed to rest for at least 1 hour at 21°C and then fertilized. Fertilized eggs were mounted in perfusion chambers (Lutz and Inoue, 1986) and were observed by epifluorescence, Differential Interference Contrast (DIC) or confocal microscopy as described by Roegiers et al. (1995).

### Micromanipulations

In order to carry out micromanipulations, egg batches with pronounced contraction poles or vegetal buttons were selected. For the ablations we used hand-pulled 100 µl pipettes with fine tips, attached to mouth pipettes. A Singer micromanipulator was used to position the micropipette under a stereomicroscope. Eggs were oriented with the contraction pole or vegetal button facing the tip of the micropipette. Parts or all of the protrusions were rapidly aspirated by capillary action or light suction. To prevent removal of excess cytoplasm, the pipette was rapidly moved once the contraction pole or vegetal button was in the pipette. This movement caused the pinching off of the fragment from the egg. The fragment was blown out of the pipette by gentle pressure and recovered. The size of each fragment was measured with a micrometer to determine its volume. Ablated embryos were allowed to develop in isolation and were either observed throughout development or fixed and labelled with antibodies or histochemically as described below.

### Treatment with cytoskeletal inhibitors

To disrupt actin microfilaments or microtubules, eggs were incubated in Cytochalasin B (2 µg/ml) or Nocodazole (1.2 µM) in TAPS SW for 12–14 minutes after fertilization.

### Labelling of fixed eggs

Zygotes or embryos either fixed for whole mount or sections were immunolabelled with mouse anti neurofilament antibody (NN18 or neurofilament 166, ICN), mouse anti-β-tubulin antibody (Amersham), or rat YL anti β-tubulin essentially as described by Sawada and

Schatten (1988); Swalla et al. (1991); Sardet et al. (1992). The antibodies were diluted 1/500 to 1/1000 in PBS with BSA (0.5%). Antibodies were detected with biotin anti-mouse/Streptavidin Texas red (Amersham) or goat anti-rat Texas red (Immunotech/Jackson). Hoechst 33342 was used to reveal the position of the male and female nuclei (Roegiers et al., 1995). Microfilaments were labelled using Rhodamine-phalloidin as described by Roegiers et al. (1995).

The presence of epithelial cells in ablated embryos was determined by examination of the surface morphology of fixed embryos. Muscle differentiation was evaluated using the acetylcholinesterase assay as described by Whittaker (1973).

### Electron microscopy

Thick and thin section electron microscopy of eggs properly oriented to observe male and female pronuclei or the vegetal button were done exactly as described by Gualtieri and Sardet (1989) and Sardet et al. (1992).

### Video, digital epifluorescence, and confocal microscopy

For video-enhanced microscopy observations, we used a Zeiss Axiophot microscope equipped with Newicon and SIT cameras (Lhesa and Hamamatsu). The images (low light fluorescence or DIC) were processed through a video processing unit (Matrox card installed in an HP 386 PC with Universal imaging software: Image 1) recorded on optical disc (Panasonic OMDR 2026) and analyzed with Universal Imaging software (Metamorph v 2.76).

For in vivo observations of microtubule and centrosome dynamics we used a Zeiss Axiovert microscope equipped with a 12 bit cooled CCD camera (Princeton Inst.), a XYZ motorized stage and filter wheel (Ludl) run by Universal imaging software (Metamorph v2.76). We acquired z series and performed subsequent image processing with Metamorph and the Exhaustive Photon Reassignment (EPR) software from Scanalytics (Billerica, MA). To reveal centrosomes in Rhodamine-tubulin-injected fertilized eggs, a series of filters were applied to successive images. For analysis of bead movement shown in Fig. 9, three images were taken every 5 seconds: one transmitted light image, one image of labelled myoplasm (Mitotracker), and one image of FITC fluospheres. These different images were stored on the computer hard disk, and later overlaid.

Confocal laser scanning microscopy was performed on a Leica confocal microscope equipped with an argon/krypton laser. For observations of living eggs stained with DiOC<sub>2</sub>(3) or DiIC<sub>16</sub> images were stored on the computer hard disk. Observations of the ER network (with DiIC<sub>16</sub>) and myoplasm (with DiOC<sub>2</sub>(3)) were performed in the simultaneous scan mode.

### Calcium imaging

Calcium ratio imaging with Calcium green dextran/Texas red dextran (Molecular Probes) was performed as described (McDougall and Sardet, 1995). Luminescence measurements of aequorin-injected eggs were acquired using the methods previously described (Speksnijder et al., 1990a).

### Fluorescence intensity measurements

A confocal image series (z-step: 2 µm) of fixed or live 16-cell embryos labelled with the NN18 antibody or with DiOC<sub>2</sub>(3), respectively, were analyzed by measuring the fluorescence intensity in individual blastomeres. A threshold fluorescence value was defined to eliminate background signal. The contour of each blastomere was visually delineated, and fluorescence intensity of each z section in the delineated region was collected for each blastomere and summed. The total fluorescence intensity of the embryo was taken as the sum of the fluorescence intensity of the complete threshold image stack. The percentage of fluorescence intensity in each blastomere was obtained from the ratio of the fluorescence intensity of the blastomere over the fluorescence intensity of whole embryo. Blastomeres which were below threshold intensity were counted as zero.

## RESULTS

### A definition of the myoplasm as a cytoplasmic domain

The myoplasm has been loosely defined as a cortical/subcortical region of the egg and zygote which when relocalized and/or transferred is associated with the differentiation of muscle cells. It presumably contains a muscle determinant which can be dissociated from its main components; mitochondria and vesicles, by centrifugation experiments (Conklin, 1931). Several investigators have attempted to define the composition of this layer in terms of organelles, cytoskeletal elements or specific macromolecules but some ambiguity still exists due to the various methods used to observe, manipulate, and isolate the myoplasm in different species (reviewed by Jeffery, 1995; Nishida, 1997).

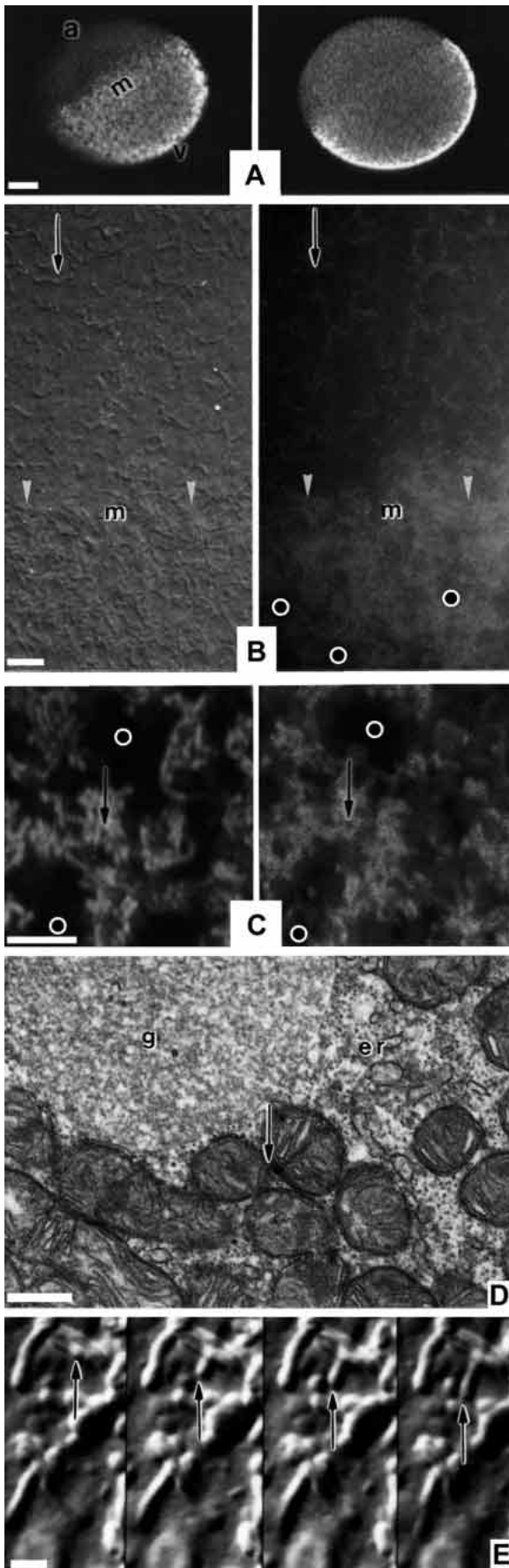
In accordance with our previous publications (Sardet et al., 1989; Speksnijder et al., 1993; Roegiers et al., 1995) we propose to call myoplasm the mitochondria-rich 6-7 µm thick subcortical layer situated beneath the 2-3 µm thick cortex of the unfertilized egg (defined as the plasma membrane and the ER and microfilament networks that tightly adhere to it; see (Sardet et al., 1992). In all species of urodele ascidians the myoplasm is characterized by a high density of tightly entangled mitochondria. In the particularly clear egg of *Phallusia mammillata* the rod-shaped mitochondria (3.5-5.5 µm) in the myoplasm can be observed in vivo (Fig. 1). The vast majority of mitochondria are immobile but in time-lapse video records individual mitochondria occasionally move (Fig. 1E). Holes through the dense mitochondrial mat provide passages to strands of the continuous ER network which extends from the cortex to the interior of the egg (Speksnijder et al., 1993) (Fig. 1B-D). Specific granules or vesicular organelles (colored yellow or orange in some species) are imbedded in the myoplasm (Fig. 1C,D). Besides being a mitochondria-rich, ER-poor cytoplasmic domain, the myoplasm in *Phallusia* is an actin-rich and microtubule-poor region (Sardet et al., 1992). It is also characterized by a meshwork of intermediate filaments previously identified in other species of ascidians (Swalla et al., 1991; Roegiers et al. unpublished).

In *Phallusia* as in other species, the myoplasm is organized as a basket with its opening in the animal pole region where the meiotic spindle lies parallel to the surface (Fig. 1A). Depending on the egg batch examined, the compactness of the mitochondria-rich domain varies, the border sometimes lying just above the equator and sometimes more than halfway up the animal hemisphere (Fig. 1A). The border area is generally well defined (Fig. 1B) and in register with the region where the continuous cortical ER network (cortical ER domain) lining the plasma membrane changes from a sparsely tubular configuration in the animal pole region to a knit configuration of tubes and sheets that become tighter in the vegetal pole region (Sardet et al., 1992; Speksnijder et al., 1993).

### Fertilization and the contraction phase (1-7 minutes after fertilization)

A spectacular cortical contraction triggered by the sperm-induced calcium wave at fertilization concentrates the subcortical myoplasm in the vegetal hemisphere (Sardet et al., 1989; Speksnijder et al., 1993; Roegiers et al., 1995). At 5-7





minutes after fertilization the zygote displays a protrusion in the vegetal hemisphere: the contraction pole (Fig. 2A,C). This contraction pole contains the bulk of the 2-6 µm thick accumulation of cortical ER, sandwiched between the center part of the myoplasmic cap and a surface zone rich in microvilli (Fig. 2B,C) (Speksnijder et al., 1993; Roegiers et al., 1995). When both ER and mitochondria are labelled and imaged simultaneously in living zygotes, an unlabelled zone (5-7 µm thick) is always detected on the cytoplasmic side of the myoplasmic layer (Fig. 2C). Upon closer examination in the electron microscope, this zone consists of an accumulation of large vesicular organelles that are most likely yolk vesicles (Fig. 2B). Thus, the cortical contraction results in the stratification of 4 distinct layers centered around the contraction pole (a surface zone rich in microvilli, the ER-rich cortical domain, the mitochondria-rich myoplasm, and the yolk-rich domain).

Micromanipulation experiments (in *Phallusia* and other ascidians), in which a large portion of the vegetal hemisphere (5-15% of egg volume) is removed with needles after fertilization, indicate that this region contains structures and/or factors that are later required for unequal cleavage division, for gastrulation, and for muscle differentiation (reviewed by Ortolani, 1958; Jeffery, 1995; Nishida, 1997). In order to ablate smaller fragments of fertilized eggs, and remove selectively the contraction pole area or part of it, we used a fine micropipette and light suction at the time the contraction pole was most prominent (5-7 minutes after fertilization). We performed 76 successful ablations of up to 5% of egg volume on various part of the egg (Fig. 2A). The 18 zygotes in which we removed less than 3% of egg volume at the contraction pole stage developed into normal tadpoles, as in unablated controls. Of the 22 cases where 3-5% of the egg volume was removed precisely at the contraction pole (see Fig. 2A, red and green circles), we obtained 3 well differentiated tadpoles (Fig. 2D), 5 grossly deformed tadpoles (Fig. 2E), and 8 amorphous cell aggregates (Fig. 2F) still containing epithelial and muscle (acetylcholinesterase positive) cells. Six operated zygotes failed

**Fig. 1.** The myoplasm: a mitochondria rich cytoplasmic domain. (A) Profile view of an unfertilized egg of the ascidian *Phallusia mammillata* whose mitochondria are labelled with DiOC<sub>2</sub>(3), observed with the confocal laser scanning microscope in tangential (left) and equatorial (right) optical sections. The border of the myoplasm (m) and the animal (a) and vegetal (v) poles are indicated. Bar, 20 µm. (B) The border of the myoplasm (m) is indicated by white arrowheads: individual subcortical rod-shaped mitochondria (arrows) in the animal hemisphere can be observed in DIC (left) and in epifluorescence when labelled with DiOC<sub>2</sub>(3). Circles (○) mark 'holes' in the dense aggregate of mitochondria. Bar, 5 µm. (C) Two confocal sections through the myoplasm close to the surface (left) and 4 µm deeper (right), showing that rod-shaped mitochondria are entangled in a continuous layer of myoplasm (arrow) interrupted by 'holes'. (Circles ○). Bar, 5 µm. (D) A thin section electron micrograph showing part of the mitochondrial layer (arrow) and part of a 'hole' where granule (g) and ER strands (er) are located. Bar, 2 µm. (E) Subcortical mitochondria in the animal hemisphere (similar to those shown by the arrow in B). They can be occasionally seen to move as in these 4 images spaced two seconds apart and extracted from a video recording (high resolution video-enhanced DIC microscopy). The arrows point to one mitochondrion moving while the others remain immobile. Bar, 2 µm.

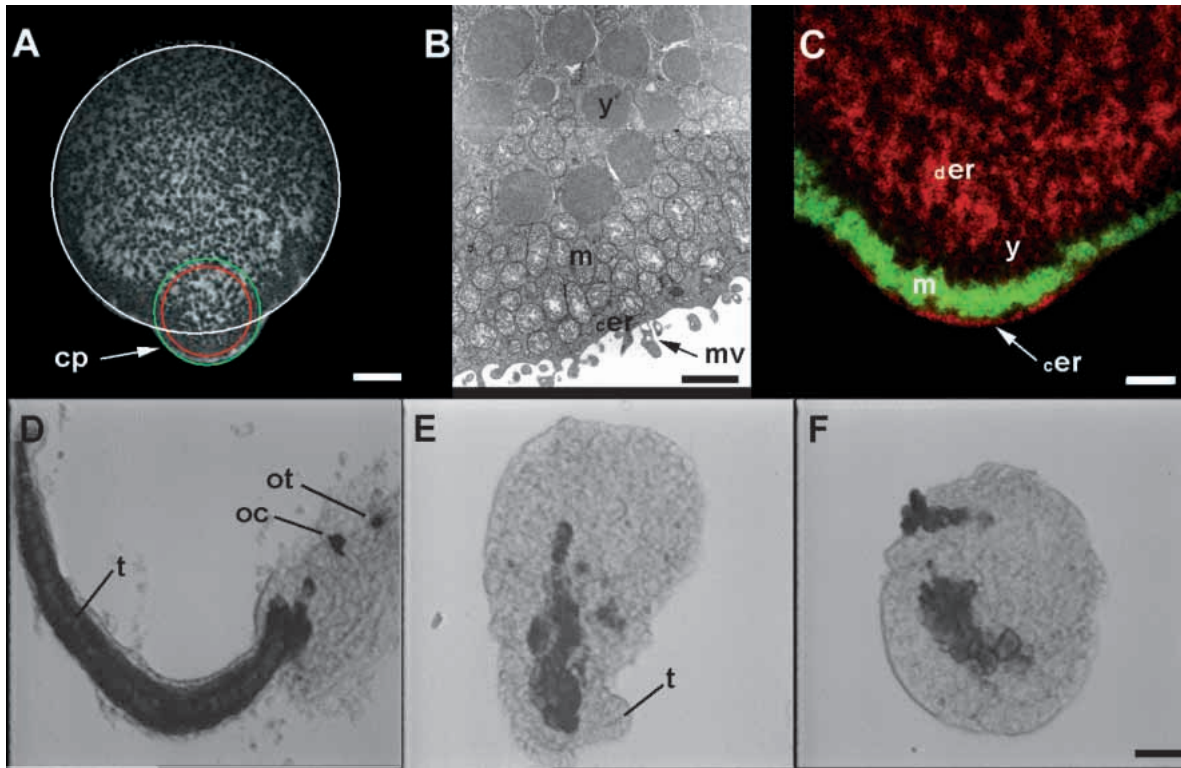


**Fig. 2.** The contraction phase (1-7 minutes after fertilization). (A) Size of ablated fragments shown on a confocal section of an egg whose ER is labelled with DiIC<sub>16</sub>. The circles drawn on the contraction pole represent the diameter of fragments removed from the contraction pole region: red circle; 3% of egg volume, green circle; 5%; white circle; 100%. Bar, 20  $\mu$ m. (B) Electron micrograph of a thin section through the contraction pole region. Four successive layers of domains are observed as in A: the yolk rich domain (y), which lies over the myoplasm (m); the cortical ER domain (cer) which is sandwiched between the myoplasm and the microvilli rich plasma membrane (mv) of the contraction pole surface. Bar, 2  $\mu$ m. (C) Composition of the contraction pole (5-7 minutes after fertilization); view of a confocal section through the contraction pole region. The egg is labelled with DiIC<sub>16</sub> to visualize ER (red), and DiOC<sub>2</sub>(3) to visualize mitochondria in the myoplasm (green). The cortical ER domain (cer; white arrow) is sandwiched between the plasma membrane and the myoplasm (m). Layered on top of the myoplasm is a yolk vesicle-rich domain (y) which contains little ER or mitochondria. The deeper cytoplasm is characterized by ER-rich (der) and ER-poor domains (see Speksnijder, 1993). Bar, 10  $\mu$ m. (D-F) Embryos resulting from ablations of the contraction pole region. The presence of acetylcholinesterase activity (black regions) indicates muscle differentiation. (D) Normal tadpole showing a fully developed tail (t) with muscle cells (black regions) and otolith and ocellus (ot and oc). (E) Grossly deformed tadpole; a small tail-like extension (t) is observed. Acetylcholinesterase activity and an ectoderm layer are present, but no other well differentiated larval structures are observed. (F) An amorphous cell aggregate. No extension of the tail is visible, and acetylcholinesterase activity is observed in small patches. Bar, 20  $\mu$ m.

to divide after the operation (presumably the male nucleus and centrosome were removed in some of these cases). When fragments with similar volumes (up to 5 %) were removed from animal or equatorial regions, zygotes developed into complete tadpoles as in unablated controls (36 cases). Although we did not carry a full analysis of cleavage patterns and of the ability of the operated zygotes to gastrulate, our experiments indicate that one can remove a large portion of the contraction pole (3% of egg volume) without adverse effect on development. We conclude that only the complete removal of the contraction pole region (5% of egg volume) and just that region starts altering axis formation and the expression of muscle cell markers.

### Oscillation and meiotic completion phase (3-25 minutes after fertilization)

Following the initial calcium wave and contraction phase a series of calcium waves cross the zygote (Fig. 3; inset) (Speksnijder et al., 1989a; McDougall and Sardet, 1995). The initiation site of the periodic calcium waves becomes permanently located in the vegetal-contraction pole where the domain of cortical ER

accumulation acts as a pacemaker (McDougall and Sardet, 1995). The contraction pole subsides about 10 minutes after fertilization (see the shape of the egg in series Aa and Ba in Fig. 3). In time-lapse video recordings, the egg is seen to oscillate until the second polar body is extruded. More specifically, each calcium wave initiated in the contraction pole region, propagates in the cortex in the animal pole direction (Fig. 3Aa,Ba), and the egg cortex constricts in the vegetal region (Fig. 3A,B). The constriction of the vegetal pole region occurs 20 to 30 seconds after the initiation of the calcium wave in the vegetal-contraction pole region and a periodic bulging of the animal pole region occurs about 10 seconds later (Fig. 3Ab,Bb). We observed the domains and the displacement of small fluorescent beads or Nile blue particles attached to the egg surface (data not shown). Whereas during the contraction phase that follows fertilization, surface particles move vegetally for distances of 70-100  $\mu$ m (Sardet et al., 1989; Roegiers et al., 1995); during the oscillation phase, surface particles move only slightly back and forth (1-2  $\mu$ m) after each passage of a wave. We conclude that during this period of repeated constrictions of the vegetal region there is no



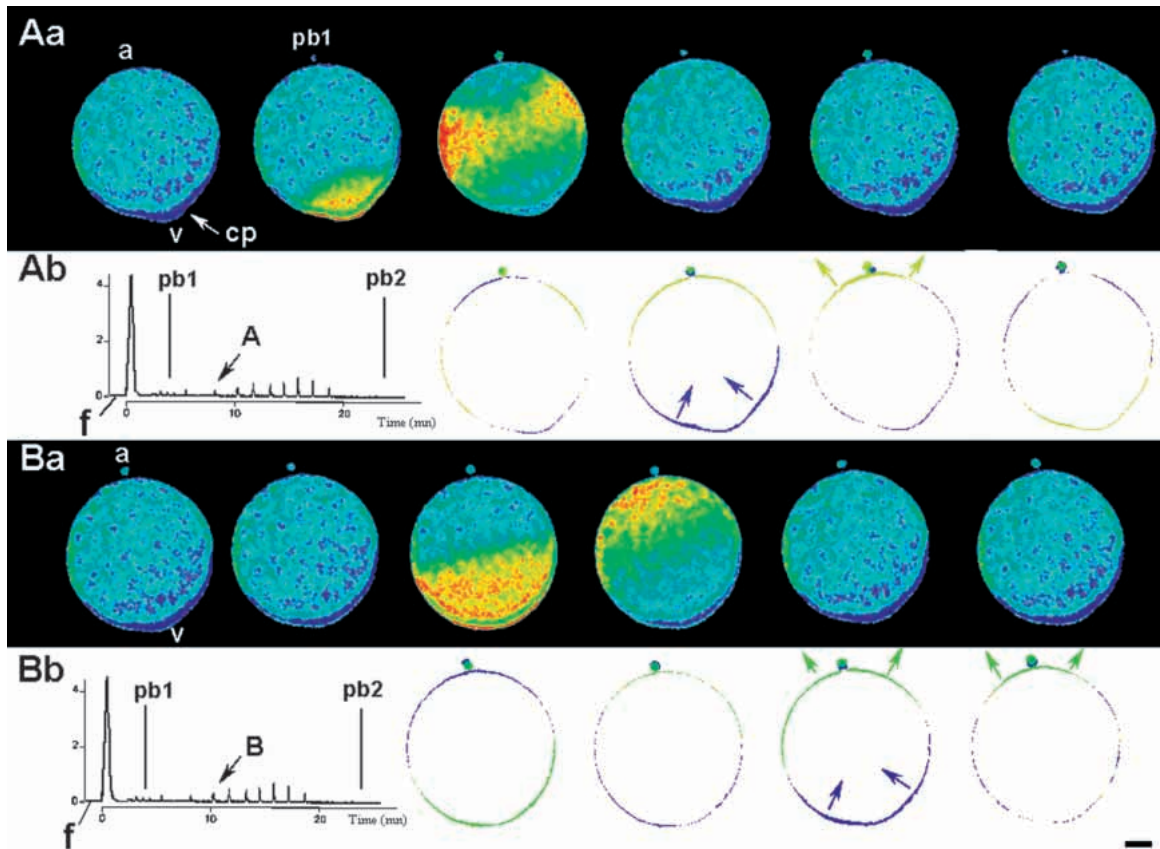


**Fig. 3.** Oscillation and meiotic completion phase (3–25 minutes after fertilization) (consult animated sequence at <http://www.obs-vlfr.fr/~biocell/BioMarCell.htm>). (Aa and Ba) Imaging of two successive oscillatory calcium waves (A and B) at 9 and 10 minutes after fertilization (see insets). In Ab and Bb, the ratio images (Calcium Green dextran/Texas Red dextran) show that the calcium waves emanate from the contraction pole. (1 image/10 second). Note that the calcium wave propagates cortically and that the contraction pole (cp) subsides after about 10 minutes. Bar, 20  $\mu$ m. (Ab and Bb) Image treatment of the ratio images shown and Ba in Aa to analyze changes in egg shape. Subtractive treatment ([image n+1]–[image n]) provides a visualization of constriction and bulging of the zygote following each calcium wave. Approximately 20 seconds after the beginning of a calcium oscillation, the contraction pole regions (cp) constricts (purple arrows). This constriction is followed ten seconds later by a bulging of the animal pole region (a) (green arrows). The insets show changes in calcium concentration obtained by luminescence intensity recordings of an egg injected with aequorin and fertilized. The large activation calcium transient is followed by a series of smaller calcium transients. The arrows show the approximate position of the calcium transients depicted in Aa and Ba (f; fertilization, pb1; first polar body, pb2; second polar body).

major displacement of the 4 domains layered in the vegetal region.

The oscillatory phase ends abruptly about 25 minutes after fertilization. The periodic calcium waves and constrictions cease and the second polar body is extruded, signaling the end of meiosis. The zygote flattens in the animal-vegetal direction (Fig. 4A, 25 minutes).

### The vegetal button stage (25–35 minutes after fertilization)

The vegetal button is a transient surface protrusion that appears in the vegetal hemisphere at the end of meiosis in the same location as the contraction pole that appeared earlier (Sardet et al., 1989; Roegiers et al., 1995 and Fig. 4A; 29 minutes, white arrow). The size and visibility of the vegetal button varies between egg batches. The vegetal button persists during most of the pronuclear migration period described below (10 minutes) and generally subsides before the pronuclei meet (Fig. 4A, 40 minutes). The vegetal button surface is characterized by numerous microvilli which remain on the

surface after the disappearance of the protrusion (Fig. 4B; 36 minutes). Microfilaments appear essential for the formation of the vegetal button since treatment with Cytochalasin B, 10 minutes after fertilization (during the oscillation phase) blocks the formation of a protrusion (Fig. 4C). In contrast, microtubules do not appear to be necessary for the formation of the vegetal button. Zygotes treated with Nocodazole, 10 minutes after fertilization, at doses that block the growth of the sperm aster, form normal vegetal buttons (Fig. 4D). However, re-absorption of the vegetal button is generally delayed by a few minutes after Nocodazole treatment.

At the time the translucent vegetal button forms, the vegetal region retains the stratified organization in layers acquired during the contraction phase (Fig. 5A,B). Electron microscopy analysis reveals that the vegetal button proper contains 3 components; the microvilli-rich surface, a portion of the cortical ER domain, and a new identifiable domain containing aggregates of dense granules (Fig. 5B,C). The structure and position of this additional domain, which we call the 'vegetal body', is reminiscent of the 'nuage' ribonucleoprotein material

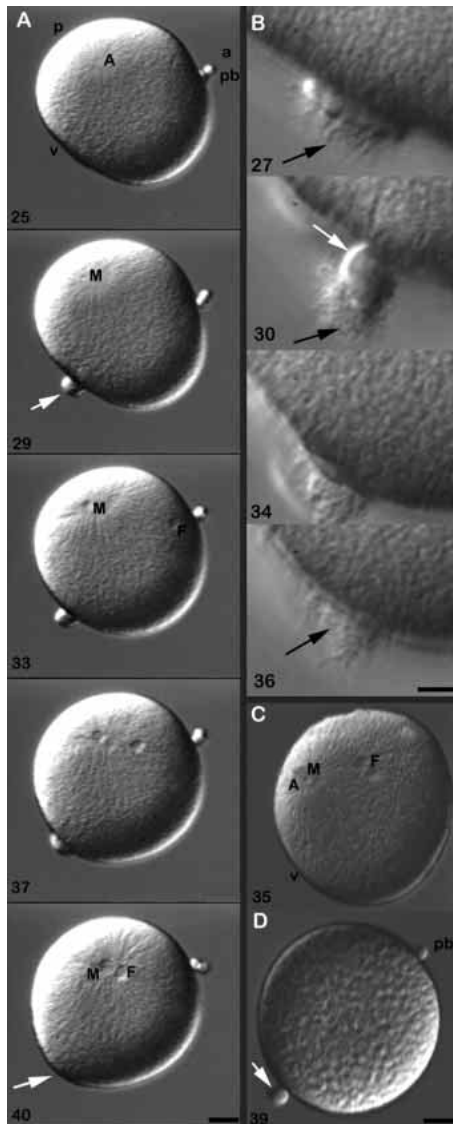


**Fig. 4.** The vegetal button stage (30–40 minutes after fertilization) (consult animated sequence at <http://www.obs-vlfr.fr/~biocell/BioMarCell.htm>). (A) Images extracted from a time-lapse series using DIC optics. The sequence begins with the extrusion of the second polar body (pb) (25 min.) and ends when the vegetal button subsides (40 minutes, white arrow). In this and all subsequent figures, times are indicated in the lower left corner of each image and represent minutes after fertilization. Bar, 20  $\mu$ m. (25 minutes) A fertilized egg at the time of extrusion of the second polar body (pb) at the animal pole (a). The sperm aster (A) has formed defining the future posterior pole (p) of the embryo. The vegetal button emerges in the vegetal pole area (v). (29, 33 and 37 minutes) Vegetal button formation and pronuclear migration. The vegetal button (white arrow) forms in the vegetal pole region shortly (1–2 minutes) after the extrusion of the second polar body. The male (M) and female (F) pronuclei form and the female pronucleus begins to migrate toward the aster. (40 minutes) The vegetal button (white arrow) begins to subside as the male (M) and female (F) pronuclei approach. (B) High resolution view of the vegetal button using DIC optics: The vegetal button first appears as a flattened protrusion with an accumulated tuft of microvilli (27 minutes black arrow). The protrusion (30 minutes white arrow) reaches its maximum 3 minutes later, the microvilli are still prominent. As the vegetal button subsides the accumulation of microvilli remains (36 minutes; black arrow). Bar, 10  $\mu$ m. (C,D) Effect of cytoskeletal inhibitors on the vegetal button. (C) In Cytochalasin B-treated eggs (1  $\mu$ g/ml), no vegetal button appears in the vegetal region (v). The sperm aster (A) is visible as well as the two pronuclei (M, F). (D) In Nocodazole-treated eggs (1.2  $\mu$ M), the vegetal button is prominent (white arrow), but the sperm aster does not form. (polar body: pb). Bar, 20  $\mu$ m.

found associated with the germ plasm in many organisms (Eddy, 1975). The results of immunocytochemistry and ablations of the vegetal button which will be reported in full elsewhere also indicate that the vegetal body of the ascidian zygote may contain germ plasm (C. Djediat, F. Roegiers and C. Sardet, in preparation)

#### Pronuclear migration phase (29–40 minutes after fertilization)

Two to four minutes after the extrusions of the vegetal button and the second polar body, nuclear membranes form around the male and female chromosomes and the pronuclei become visible (Fig. 4A). We have analyzed the duplication, separation and positioning of centrosomes from through-focus image series of eggs injected with Rhodamine tubulin prior to fertilization (Fig. 6A). At the end of the meiotic period, a single centrosome is observed in the center of the astral region (Fig. 6A, 23 minutes). It duplicates, and two centrosomes are always distinguished when the egg extrudes its second polar body (Fig. 6A, 25 minutes). The duplicated centrosomes separate in a direction perpendicular to the animal vegetal axis (Fig. 6A). As

a consequence the aster changes its shape from a sphere to a disk and its central region elongates. The centrosomal region concentrates refractile dense bodies within the smooth astral region which is rich in ER and microtubules (Fig. 6B, 29–31 minutes see also Fig. 7A,C). This dense body material probably represents the accumulations of membranes and annulate lamellae seen with the electron microscope (Fig. 6D).

As expected, centrosome separation is inhibited in zygotes treated with Nocodazole where a single centrosome remains in the center of a much reduced astral region (data not shown). We observed similar microtubule patterns in both fixed preparations labelled with anti-tubulin and in live eggs injected with Rhodamine tubulin (Fig. 6C). At first, the aster is a radial accumulation of microtubule bundles emanating from a small spherical centrosomal region in a subcortical location (Fig. 6C, 25 minutes). The microtubules at this stage appear not to invade the animal pole area. After centrosome duplication, the central astral region elongates and the density of microtubule bundles increases in a direction perpendicular to the animal vegetal axis (Fig. 6C, 29 minutes). Astral microtubules lengthen in all directions reaching the animal pole area and the multi-lobed female pronucleus (Fig. 6B, 36 minutes).

#### The slow posterior translocation phase (25–40 minutes after fertilization)

At the time the multi-lobed female pronucleus starts its migration towards the center of the sperm aster, the posterior portion of the egg assumes characteristic morphological features and motions. We have analyzed these events using a combination of light, confocal and electron microscopy techniques (Fig. 7). The male pronucleus, which has also

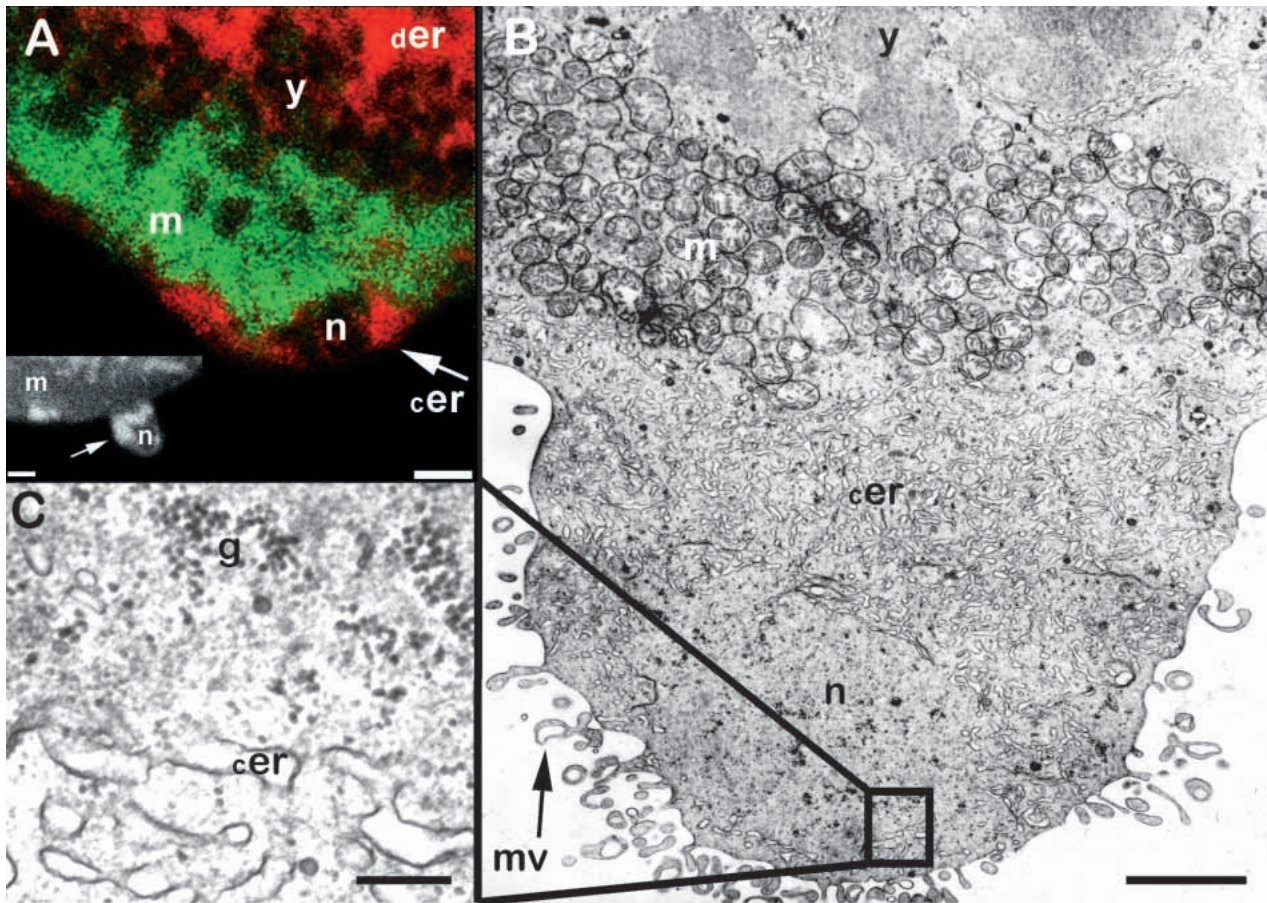


**Fig. 5.** Cortical and cytoplasmic domains in the vegetal pole region during the vegetal button stage (30-40 minutes after fertilization). (A) Distribution of ER and mitochondria in the vegetal button. A confocal section of the vegetal button in an egg injected with DiIC<sub>16</sub> and DiOC<sub>2</sub>(3) to label cortical (cer) or deeper (der) ER (red) and mitochondria (green), respectively. In this highly compressed zygote an accumulation of ER (white arrow) surrounds an unlabelled region (n) which corresponds to the 'nuage-like' material seen in B (see below). The myoplasm layer (m) lies above the vegetal button region. The yolk-rich domain (y) is still present on the cytoplasmic side of the myoplasm. Bar, 5  $\mu$ m. Inset: a confocal section of a vegetal button in a less compressed zygote labelled with DiIC<sub>16</sub> to visualize ER. The protruding vegetal button contains only ER (white arrow) and the nuage-like (n) material. Bar, 10  $\mu$ m. (B,C) Electron micrograph of an ultra-thin section through the vegetal button. It shows the yolk-rich domain (y) and the dense accumulation of mitochondria which corresponds to the myoplasm (m). Below the myoplasm layer the cortical ER domain (cer) surrounds the 'nuage-like' material (n) which contains numerous electron dense granules (g) (see inset, Bar, 0.3  $\mu$ m). Microvilli (mv) protrude from the surface of the vegetal button. Bar, 2  $\mu$ m.

started to migrate, is flanked by trails of ER-rich domains (Fig. 7A,C). These trails contain bundles of microtubules emanating from the duplicated centrosomes (Fig. 7B and live observations with Rhodamine tubulin not shown here). Some of these astral microtubules course along the posterior cortex (Fig. 7B). In contrast to the ER-rich domains which contain most microtubules, the mitochondria-rich myoplasm tightly apposed to the posterior side of the male pronucleus has few microtubule bundles (Fig. 7B).

The posterior cortex during this period is highly active; it vibrates at high frequency deforming the egg surface (Fig. 7D). This vibratile activity is abolished by Nocodazole treatment. A slow translocation of the myoplasm and cortical ER domain starts with a slow and discontinuous motion of the pronuclei towards each other (Sardet et al., 1989). Observations of the myoplasm at this time show that it has started to rearrange (Fig. 8A, 25-28 minutes). The first sign of change is that the cup-shaped myoplasmic layer folds in its center (Fig. 8A, 28

minutes). This may be related to the re-absorption of the vegetal button.

#### The fast posterior translocation phase (40-45 minutes after fertilization)

The slow phase of translocation associated with the vibratile activity of the posterior cortex is followed by a fast phase of translocation (Sardet et al., 1989). This involves, the duplicated male centrosome and associated asters, the adjoining male and female pronuclei as well as the ER-rich and mitochondria-rich domains, all moving towards the center of the egg (Fig. 8). At this time, a tear in the myoplasmic layer becomes apparent in the vegetal pole area (Fig. 8A, 37-41 minutes, Fig. 8B, 39 minutes).

During the fast microtubule-driven motion, the bulk of the myoplasm folds and translocates posteriorly (Fig. 8A, 37-41 minutes). Part of it moves to the center of the egg as if tethered to the male pronucleus while most of the myoplasm folds upon



itself in a posterior vegetal location (Fig. 8A, 41 minutes). Because of the tear in its vegetal region a small amount of myoplasm in the lateral and anterior parts of the egg forms a subequatorial girdle (Fig. 8A, 37-41 minutes, Fig. 8B, 39-41 minutes). We had observed previously that the bulk of the domain of cortical ER accumulation at the vegetal-contraction pole translocated posteriorly at about the same time as the myoplasm (Speksnijder et al., 1993). In confocal sections of properly orientated zygotes in which ER and mitochondria are labelled simultaneously it can be observed that the movements of the myoplasm and ER-rich cortical domains occur in concert and without significant mixing (Fig. 8C, 23-41 minutes). In an egg that has its posterior pole oriented toward the lens, successive optical sections (2  $\mu$ m thick) reveal ER-rich columns which originate at the surface in the cortical ER domain and penetrate through the myoplasm (Fig. 8D). These ER columns presumably coincide with the passageways traversed by astral microtubules extending out to the posterior cortex.

### Mitosis and the vegetal relaxation phase (42-45 minutes after fertilization)

Once located in the center of the zygote, the male and female pronuclei lose their nuclear envelope and mitosis begins. We have observed a previously undescribed surface movement in the vegetal pole area that occurs within one minute of nuclear membrane disappearance (Fig. 9). The vegetal cortex of the zygote relaxes, such that the myoplasm moves towards its final position near the equator. This cortex relaxation can be observed with fluorescent beads or Nile blue particles attached to the egg surface (Fig. 9A,B). When the beads or particles are placed on the unfertilized egg surface in the vegetal hemisphere, they accumulate on the contraction pole after fertilization (Roegiers et al., 1995). The beads or particles remain clustered in this vegetal location until the end of the fast translocation phase. During the vegetal relaxation phase the cluster of particles or beads disperses over a broad section of the vegetal hemisphere at the same time vegetal microvilli

**Fig. 6.** The pronuclear migration phase (29-40 minutes after fertilization). (A) Centrosome duplication. Images taken from a time-lapse series of eggs injected with Rhodamine tubulin to label microtubules. The zygote is observed from the animal pole. A single centrosome is visible in the center of the aster at the end of meiosis (23 minutes, white arrowhead). As the pronuclei form, the centrosomes, which have duplicated, begin to separate (25 minutes). The intercentrosomal distance increases (29 minutes). Bar, 20  $\mu$ m. (B) Three DIC images from a time-lapse video sequence of the male centrosomal region (29 minutes). Centrosomal dense bodies can be observed in the perinuclear region (29-36 minutes, black arrows, see also D below). Formation of the pronuclear membrane (29 minutes, M) in the center of the centrosomal region. The central astral region progressively elongates (31 minutes). At the end of pronuclear migration the male (M) and multi-lobed female (F) pronuclei meet. Bar, 10  $\mu$ m. (C) Microtubule organization in live zygotes (25, 29, 33 minutes) and fixed zygotes (35 minutes) before and during pronuclear migration. Bar, 20  $\mu$ m. (25, 29, and 33 minutes) Images extracted from a confocal time-lapse sequence of a live zygote (viewed from the animal pole) injected with Rhodamine tubulin to observe microtubule dynamics. (25 minutes) Spherical sperm aster (A) with a single centrosome (white arrowhead) just after meiosis completion. (29 minutes) The sperm aster becomes asymmetrical after duplication of the centrosomes (white arrowheads). Microtubule streaks appear (white arrows). (33 minutes) The duplicated centrosomes surround the male pronucleus (M). (35 minutes) Posterior vegetal view of a fixed zygote. The zygote is fixed and labelled with an anti- $\beta$ -tubulin antibody and observed using the confocal microscope. The male pronucleus (M) is surrounded by bundles of microtubules which connect the two centrosomal regions, the cytoplasm contains a dense array of subcortical microtubules emanating from the sperm aster and extending towards the animal pole. The microtubule-poor region (m) corresponds to the translocating myoplasm. (D) Electron micrograph of centrosomal region near the male pronucleus. The male pronucleus (M), is closely associated with electron dense membranous material (cm) in the centrosomal region. This region is also rich in annulate lamellae (al). Bar, 1  $\mu$ m.

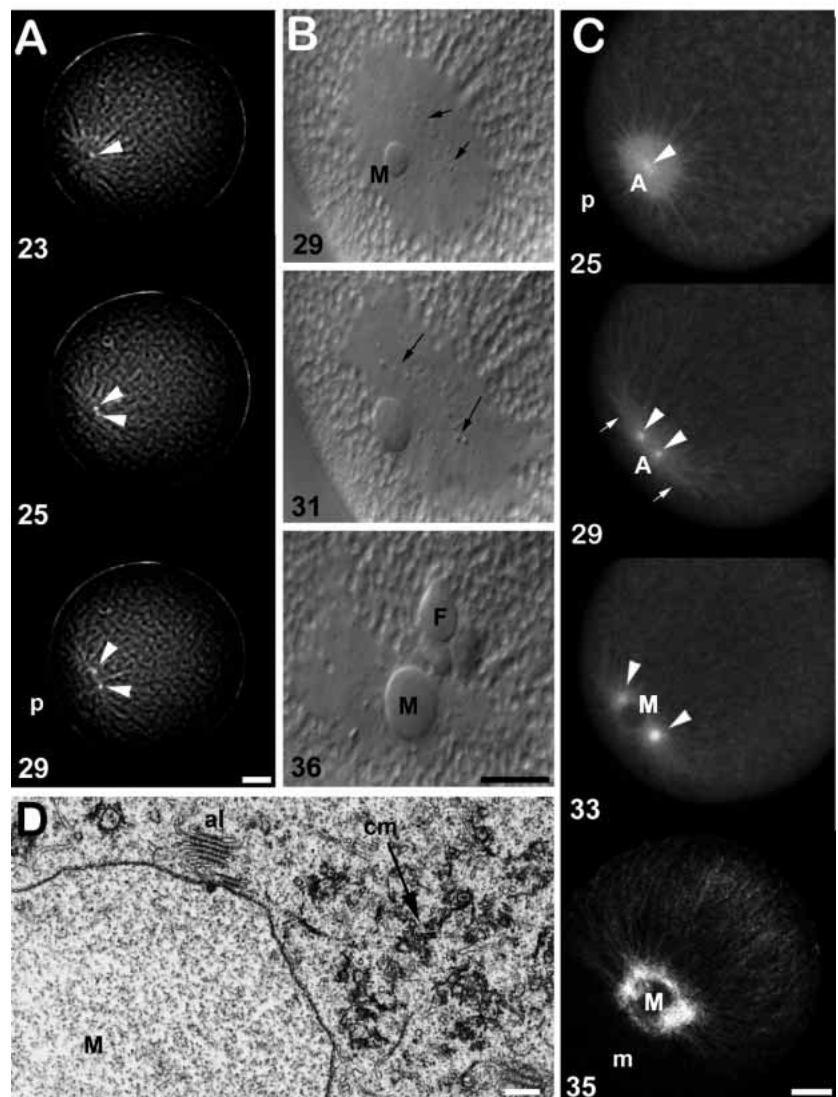
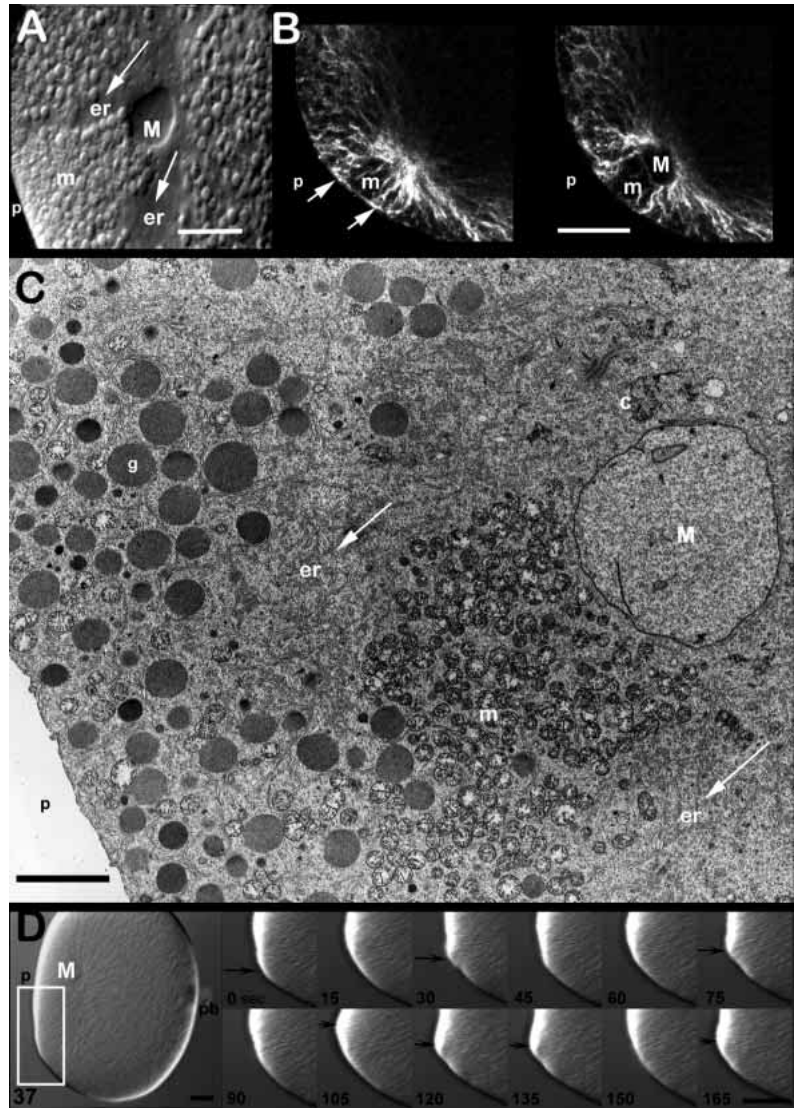


**Fig. 7.** The slow posterior translocation phase (25–40 minutes after fertilization) (consult animated sequence at <http://www.obs-vlfr.fr/~biocell/BioMarCell.htm>). (A) Image extracted from a time-lapse series of the posterior (p) region of zygote observed in DIC 34 minutes after fertilization. The male pronucleus (M) with adhering myoplasm (m) is slowly translocating along smooth regions (arrows) filled with ER (er) and microtubule bundles (astral rays). Bar, 10  $\mu$ m. (B) Serial confocal optical sections (2  $\mu$ m) of the region between the male pronucleus and the surface of the zygote (whole-mount immunolabelling with anti-tubulin). Profile view of the posterior pole (p) corresponding to those shown in A and C. The myoplasm (m) is seen as a microtubule poor region behind the male pronucleus (M) which is surrounded by microtubule-rich regions. Note also that cortical microtubules are present between the egg surface and the myoplasm (white arrows). Bar, 20  $\mu$ m. (C) Electron micrograph of an ultrathin section through the area between the surface of the zygote (posterior pole: p) and the male pronucleus (M). Distinct cytoplasmic domains are clearly visible; the myoplasm (m), ER domains (er, white arrows), an equatorial domain rich in vesicular organelles (g). Bar, 5  $\mu$ m. (D) Surface vibrations in the posterior (p) cortical region close to the sperm aster. Images taken from a time-lapse DIC series (1 image/15 seconds) beginning 37 minutes after fertilization. The deformations are visible on the image sequence (0–165 seconds) corresponding to the area indicated in the white rectangle (left image). The images have been stretched by a factor of two in the x axis to amplify deformations of the posterior vegetal pole surface which are clearly visible in accelerated time-lapse video sequences (M; male pronucleus). Bar, 20  $\mu$ m.



are re-absorbed (Fig. 9A,B). The particles slow down as they disperse away from the vegetal pole region, their average speed being in the order of 0.14  $\mu$ m/second. The spreading of surface particles lasts about 3 minutes and coincides with a final repositioning of the myoplasm towards the equator prior to anaphase.

The microfilament disrupting agent Cytochalasin B blocks the spreading of particles away from the vegetal pole (data not shown). In contrast these surface movements are not sensitive to concentrations of Nocodazole which inhibit the posterior translocation and the formation of the mitotic spindle. As mitosis proceeds, the small mitotic spindle elongates and the mitotic asters grow rapidly to spread all the way to the egg cortex with many microtubules curving along the internal surface of the cortex (Fig. 10A).

### Partitioning of cytoplasmic domains during early cleavage stages

At the end of mitosis the first cleavage furrow bisects equally the posterior domains of cortical ER and the mitochondria-rich myoplasm (Fig. 10B,C). In epifluorescence, the cortical ER domain appears either as a bar or a dumbbell sandwiched

between the plasma membrane and the central part of the posterior myoplasm (Fig. 10B). The cortical ER domain appears as a smooth patch in DIC images of dividing eggs (Fig. 10C). This smooth patch, like the vegetal button varies in size and visibility between different egg batches, and is best seen when cleavage is well advanced. The posteriorly located myoplasm and cortical ER domain do not seem to undergo major translocations during the first 2 cleavages and are allocated equally to the first 2 blastomeres. As expected from previous observations (Conklin, 1905b) the bulk of these domains is later inherited by the posterior vegetal blastomeres at stages 8 and 16. Conklin even foresaw that the 'small area of clearer protoplasm' (i.e. the accumulated layer of cortical ER) segregated to the small posterior blastomeres and the tissues that derived from them (Conklin, 1905a,b).

Because not all the myoplasm translocates to the posterior pole (Fig. 8A,B), we carried out a quantitative analysis of its partitioning into various blastomeres at the 16-cell stage. We labelled the mitochondria-rich myoplasm in live embryos with DiOC<sub>2</sub>(3) and acquired confocal z series through the embryos at the 16-cell stage (Fig. 10F). Embryos from the same batches of fertilized eggs were also fixed and labelled using NN18, an anti-

**Fig. 8.** The fast posterior translocation (40–45 minutes after fertilization). (consult animated sequence at <http://www.obs-vlfr.fr/~biocell/BioMarCell.htm>). (A) Images from a time-lapse confocal series: Median section through a zygote oriented with its animal-vegetal (v) axis and posterior pole (p) in the plane of the figure. The mitochondria are labelled with DiOC<sub>2</sub>(3) to visualize the myoplasm (green). At the completion of meiosis the myoplasm is distributed as a cup-shaped subcortical layer. Three minute later the central part of the myoplasm domain begins to fold. As the centrosomal region (c) becomes disc-like the myoplasm continues to fold (28 to 37 minutes). The myoplasm tears (arrow). The bulk of the myoplasm is drawn to the future posterior pole and to the center of the egg as the aster moves toward the egg center with the pronuclei. Some myoplasm remains on the future anterior side (a) of the embryo after a tear develops during the posterior translocation. Bar, 20  $\mu$ m. (B) The myoplasm (green) is observed in time-lapse video microscopy. Although most of the myoplasm is concentrated in the future posterior pole region (p) a girdle of myoplasm is present in a subcortical position all around the egg. Bar, 20  $\mu$ m. (C,D) Images from a time-lapse confocal series (median section). The endoplasmic reticulum labelled with DiIC<sub>16</sub> is shown in red. The myoplasm labelled with DiOC<sub>2</sub>(3) is shown in green. (C) The cortical ER domain (white arrowheads) is observed as patches between the myoplasm and the plasma membrane. The myoplasm and the cortical ER move progressively and simultaneously towards the sperm aster (A) towards the future posterior pole of the embryo (p). A large part of the cytoplasmic ER domains accumulate in the center of the sperm aster (A). (see Speksnijder et al. 1993). (D) Serial confocal sections (2  $\mu$ m) through the posterior pole region of a zygote during the posterior translocation phase. The sequence begins with a grazing section of the posterior surface of the zygote (p) and progresses 8  $\mu$ m towards the egg center through the myoplasm (m). The subcortical myoplasm (green) is traversed by corridors of ER (red) extending from the astral region to the cortex. Bar, 20  $\mu$ m.

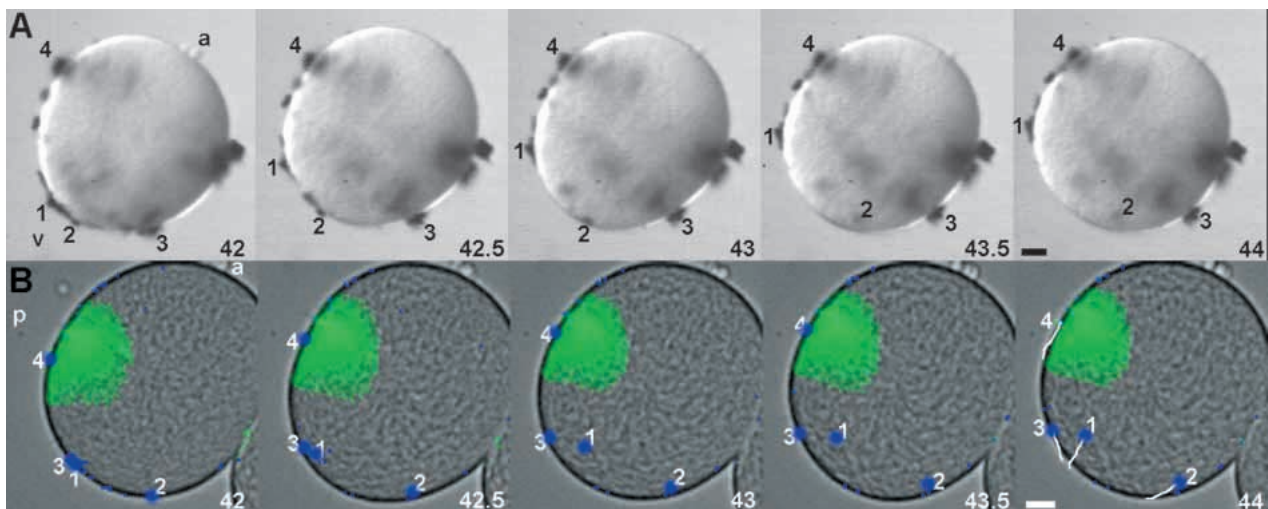
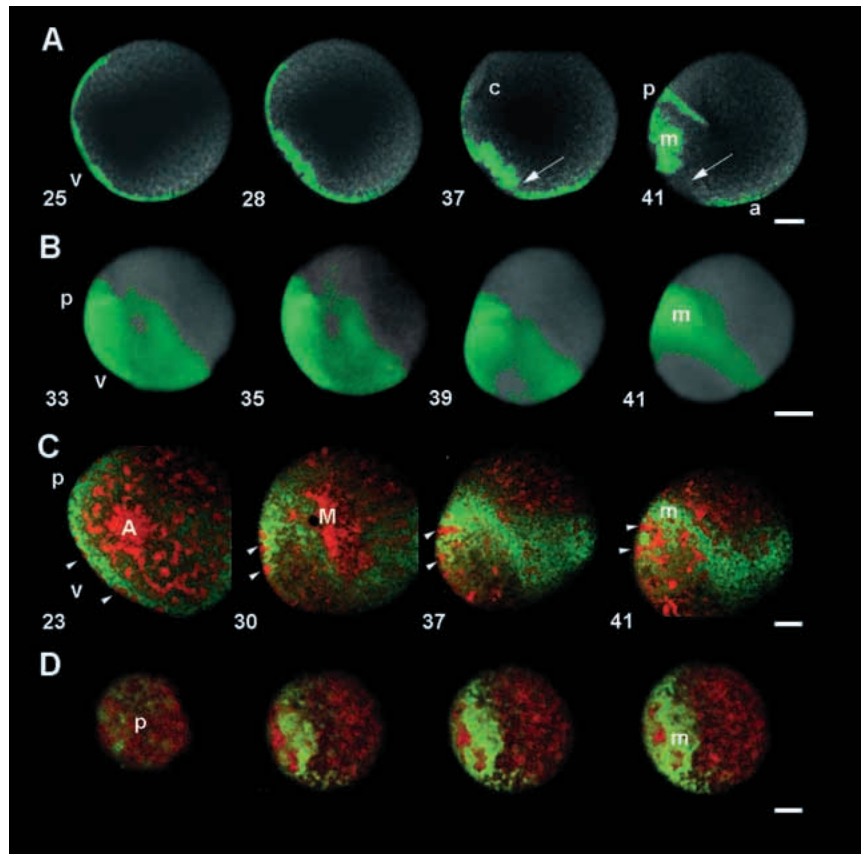


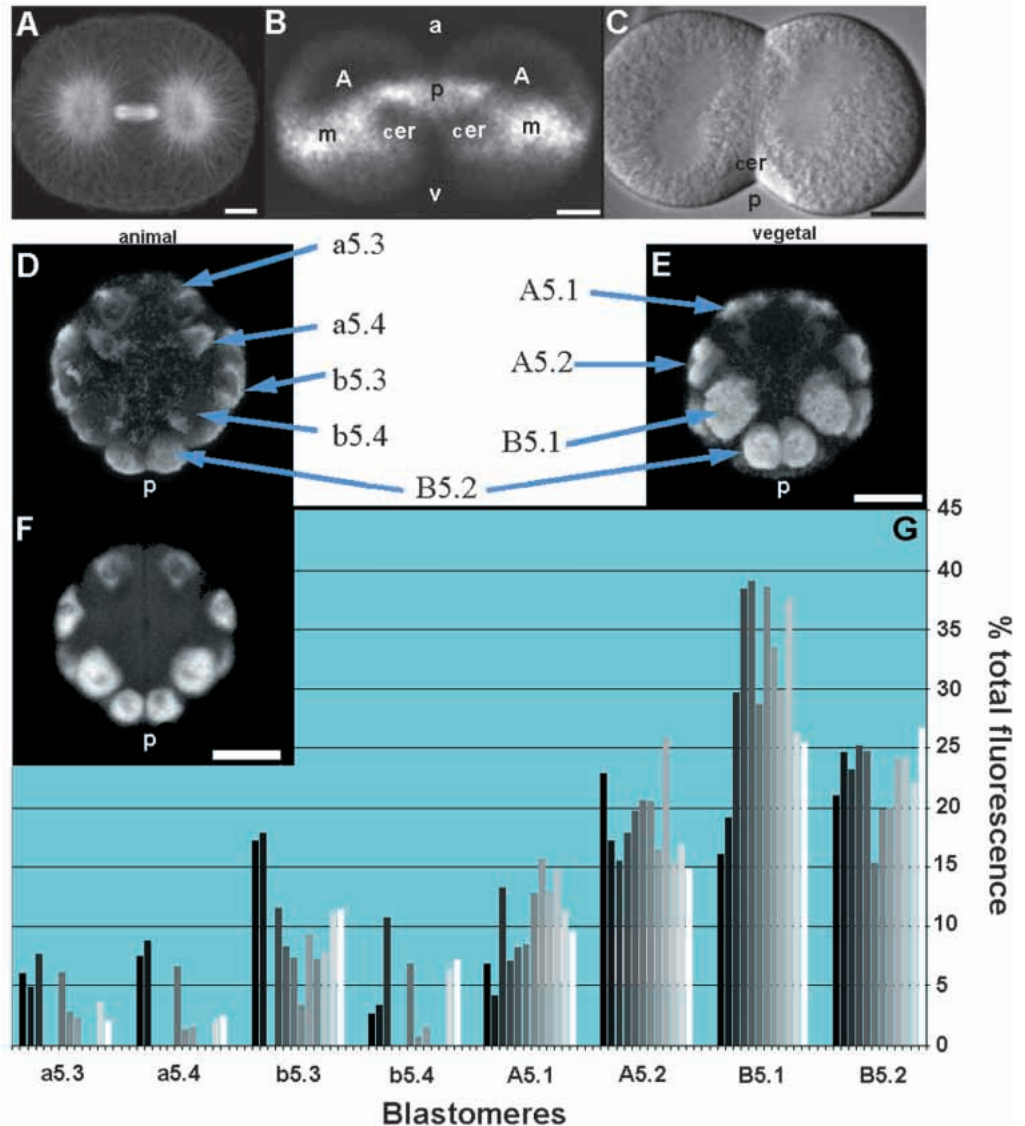
**Fig. 9.** Vegetal relaxation phase (45–47 minutes after fertilization) (consult animated sequence at <http://www.obs-vlfr.fr/~biocell/BioMarCell.htm>). (A) Images extracted from a video time-lapse record of a zygote labelled with Nile blue particles 42 minutes after fertilization. The particles close to the vegetal pole (v) region move towards the equator. In this sequence particle 2 moves out of the plane of focus, while 1 and 3 move in the plane of focus out of the vegetal pole. Particle 4 in to the animal hemisphere (a) does not move appreciably during this phase. Bar, 20  $\mu$ m. (B) Time-lapse sequence of a zygote simultaneously labelled with Mitotracker to follow movements of the myoplasm (green), and fluorescent carboxylate beads (blue dots) to follow surface movements. Beads 1 and 3 clustered at the vegetal pole (v) begin to disperse equatorially within two minutes. Bead 4 affixed to the posterior egg surface (p) adjacent to the myoplasm move with it in the animal pole direction. The trajectories of beads 1, 2, 3, 4 between 42 and 44 minutes are shown as white lines in the last image (44 minutes). Bar, 20  $\mu$ m.



**Fig. 10.** Distribution of the myoplasm at the 16-cell stage.

(A) Mitotic spindle: The mitotic spindle visualized in a fixed zygote using an anti- $\beta$ -tubulin antibody. Note the large asters with astral rays reaching the cortex. Bar, 20  $\mu$ m. (B) Myoplasm and cortical ER at the 2-cell stage. Posterior view of a cleaving egg labelled with DiOC<sub>2</sub>(3) to visualize the myoplasm (m). Astral regions are seen as dark areas (A). The cortical ER domain also appears as a dark region dumbbell-shaped (cer). Bar, 20  $\mu$ m. (C) A DIC image of a cleaving egg seen from the vegetal pole. The cortical ER (cer) domain appears as a smooth patch in the posterior region (p). Bar, 20  $\mu$ m. (D,E) Distribution of the myoplasm in 16-cell stage embryos labelled with the NN18 antibody, a marker for intermediate filaments in the myoplasm. Images D and E are projections views from series of optical sections taken through a 16 cell embryo stained with the NN18 antibody. (D) An animal pole view showing that some labelling of the myoplasm occurs in animal blastomeres (a5.3, a5.4, b5.3, and b5.4). (E) A vegetal pole view showing that the strongest accumulation of myoplasm is in the A5.2, B5.1, and B5.2 posterior (p) blastomeres. (B5.1 and B5.2 blastomeres will give rise to the primary tail muscle lineage). Bar, 50  $\mu$ m. (F) A single plane from a series of confocal optical sections taken through the vegetal

blastomeres of a living 16 cell embryo stained with DiOC<sub>2</sub>(3) which labels mitochondria and the myoplasm. Bar, 50  $\mu$ m. (G) The relative distribution of myoplasm measured from fluorescent intensity measurements in the blastomeres of 12 different embryos (16-cell stage). Each bar (from left to right) represents the percentage of myoplasm per blastomere of a single embryo. The position and shading of the bars indicate the measures made on the different blastomeres of a single embryo (i.e. first black bar on the left corresponds to the same embryo).



human neurofilament antibody that recognizes an epitope in the myoplasm (Fig. 10D,E; Swalla et al., 1991). Similar distributions of myoplasm between the different blastomeres were deduced using these two techniques. The results of our analysis are shown in the graph in Fig. 10. Although the posterior blastomeres contain the bulk of the myoplasm (B5.1: 30% and B5.2: 22%) both anterior vegetal blastomeres contain a significant amount of myoplasm (A5.2: 18% and A5.1: 10%). In contrast, the animal blastomeres contain smaller amounts of myoplasm (b5.4: 3%, b5.3: 9%, a5.3: 3% and a5.4: 2%). Thus as Conklin and others demonstrated the different phases of relocalization result in locating the bulk of the myoplasm in the vegetal posterior blastomeres, which differentiate into the primary muscle cells of the tadpole's tail (Conklin, 1905b; Reverberi, 1956; Zalokar and Sardet, 1984; Satoh, 1994). However as suggested earlier (Sardet et al., 1989), a significant proportion of the myoplasm is also

inherited by the anterior vegetal and posterior animal blastomeres, at the 16-, 32- and 64-cell stage. These blastomeres give rise to endodermal and mesodermal structures, including secondary muscle cells (Nishida and Satoh, 1985; Meedel et al., 1987; Venuti and Jeffery, 1989).

## DISCUSSION

It has generally been considered that the ascidian egg undergoes two main phases of reorganization (or 'ooplasmic segregation') between fertilization and first cleavage. Our detailed studies using the transparent egg of the ascidian *Phallusia mammillata* reveal that these two major phases (gray areas in Fig. 11) are only parts of a succession of numerous phases and events outlined in the upper part of Fig. 11. The

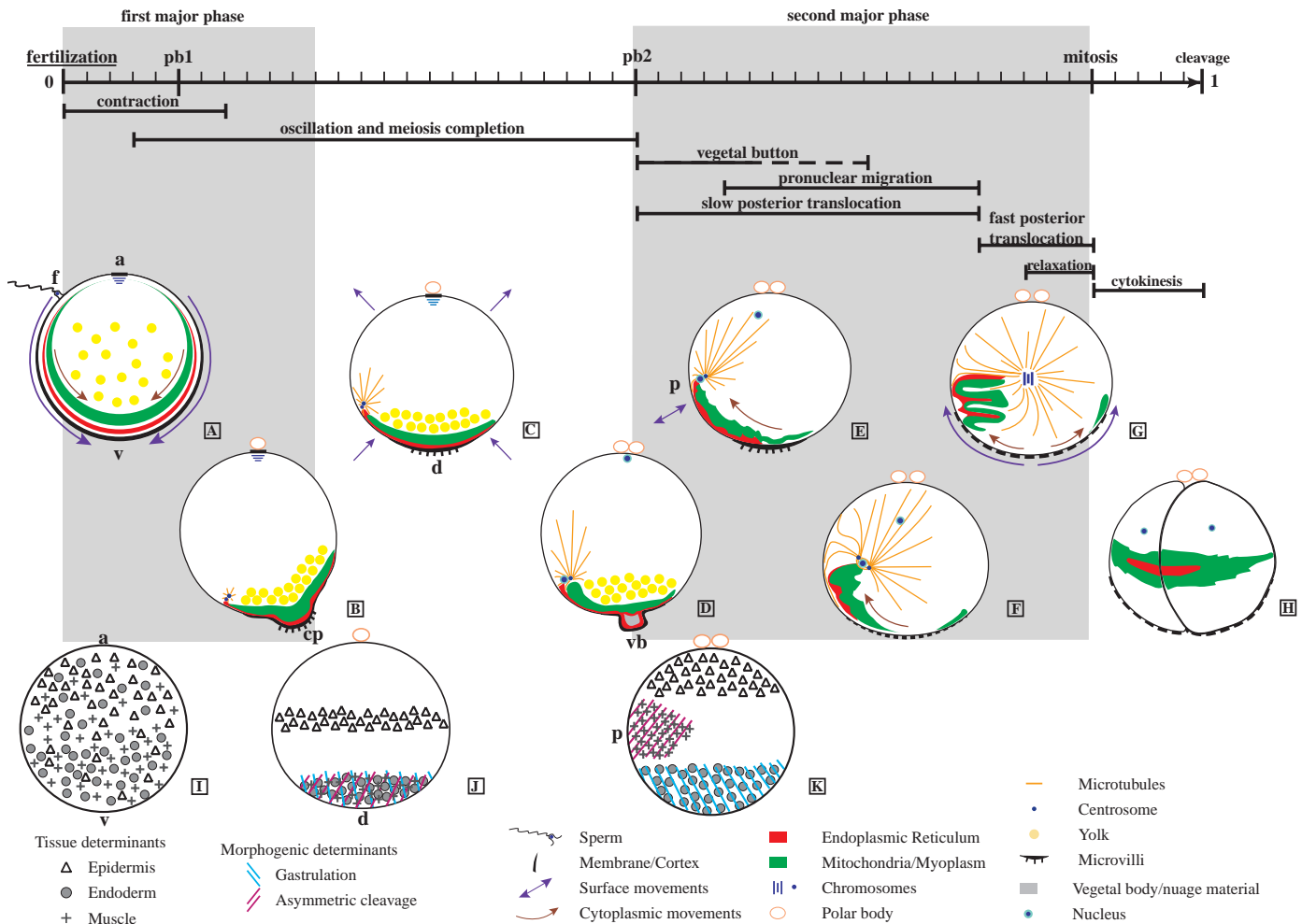


**Fig. 11.** Events and phases of cortical and cytoplasmic reorganizations in the ascidian zygote (see Discussion for detailed legend). The drawings represent in an exaggerated manner the phases of reorganizations of the surface (black outline) the cortical reticulum (red), the myoplasm (green) and some yolk vesicles (yellow) between the events of fertilization and cleavage. The microtubules, centrosomes, chromosomes and nuclei are also represented. The deeper organelles and endoplasmic reticulum are not represented. Arrows facing inside and outside indicate coordinated movements while arrows perpendicular to the surface indicate constriction, bulging or vibrations of the surface. The gray areas represent the first and second major phases of reorganization. The diagrams (I,J,K) are schematic representations of the relocalization of putative morphogenetic determinants and determinants for the differentiation of tissues (redrawn according to Jeffery, 1995 and Nishida, 1997).

middle part of Fig. 11 is a schematic representation of the surface, cortical and cytoplasmic reorganizations of the domains identified in this and previous reports. We first go through a description of these changes and then compare them to the reorganizations observed in other eggs.

### I: Successive phases of surface, cortical and cytoplasmic reorganization:

Reorganizations in the ascidian zygote (read as the detailed legend of Fig. 11; the events and phases are underlined)

The mature ascidian oocyte, arrested in metaphase I of the meiotic cell cycle is radially symmetrical around an animal-vegetal axis (a, v) established during oogenesis (Sato, 1994; Jeffery, 1995). The small meiotic spindle lies parallel to the animal pole cortex (Fig. 11A). Lining the rest of the cortex is a polarized thin layer of microfilaments and cortical ER network as well as a basket of subcortical myoplasm (black,

red and green zones respectively in Fig. 11A) (Sardet et al., 1992). The sperm usually fertilizes the egg in the animal hemisphere and locally triggers a calcium wave that propagates through the egg (Fig. 11A) (Speksnijder et al., 1989b; Brownlee and Dale, 1990; Speksnijder et al., 1990a). This represents the initial symmetry breaking event and the signal for the egg to re-enter the meiotic cell cycle. The zygote then proceeds through a succession of stereotyped phases of cortical and cytoplasmic reorganizations in register with the temporal and spatial events of the meiotic and first mitotic cell cycle.

Fertilization causes the first major reorganization: the contraction phase (Fig. 11A,B). It is a spectacular contraction of the cortex and subcortex that propagates vegetally which stratifies and concentrates at least 4 surface, cortical and subcortical cytoplasmic domains into layers centered around the contraction pole (cp) in the vegetal pole region (Fig. 11B). A new yolk-rich domain (yellow dots) can be discerned at this time. In *Phallusia*, the exact location of the contraction pole

depends on the site of sperm entry and prefigures the site of gastrulation and the location of the dorsal side (d) of the embryo (Roegiers et al., 1995). This contraction also moves the sperm nucleus and centrosome to a subcortical location in the vegetal hemisphere (Speksnijder et al., 1989b; Roegiers et al., 1995). This site will determine the future posterior side (p) of the embryo (Fig. 11E) (Conklin, 1905b). The contraction pole re-absorbs after the first polar body is emitted and the zygote enters the oscillatory and meiotic completion phase (Fig. 11C). For about 20 minutes the vegetal-contraction pole region constricts periodically with respect to the onset of each calcium wave initiated in the cortex of the contraction pole. No apparent relocalization of stratified domains occur at this time. The waves and oscillations then cease, signaling the end of the meiotic cell cycle (Speksnijder et al., 1990b; McDougall and Sardet, 1995; Russo et al., 1996; Yoshida et al., 1998). The animal pole cortex emits the second polar body and the vegetal pole cortex a local protrusion: the vegetal button (vb) (Fig. 11D). An additional cytoplasmic domain the 'vegetal body' (gray area) is detected in the vegetal button region.

During the vegetal button stage nuclear membranes form around the male and female chromosomes (Fig. 11D). The pronuclear migration phase starts (Sawada and Schatten, 1988; Sardet et al., 1989; Sawada and Schatten, 1989). The paternal centrosome duplicates and the growing astral region stretches into an elongated disc. The astral microtubules are located in ER corridors and grow into the cortical ER layer along the cortex traversing the myoplasm (Fig. 11E). We suggest that the interplay between the posterior cortex and the astral microtubules cause the posterior region of the cortex to vibrate (Fig. 11E). A slow translocation phase ensues; the female pronucleus migrates towards the center of the paternal aster, the myoplasmic cap in the vegetal region fold and is slowly and discontinuously displaced in the posterior direction until it finally tears (Fig. 11F). The astral microtubules then glide (and possibly grow) along the cortex pushing the asters and pronuclei away from their subcortical location and towards the center of the zygote. During this fast translocation phase the bulk of the myoplasm and cortical ER domains are displaced without mixing towards the posterior pole and center of the zygote but there are no surface movements (Fig. 11F). Male and female pronuclei and centrosomes have now relocated to the center of the zygote forming a small mitotic spindle and two very large asters extending their microtubules along the cortex (Fig. 11F). Mitosis and the vegetal relaxation phase complete the final relocalization of cortical and cytoplasmic domains (Fig. 11G). A wave of cortical relaxation starts in the vegetal pole region at metaphase of mitosis. It spreads out the tuft of microvilli in the vegetal cortex and moves the myoplasm to a more equatorial position (Fig. 11G). During cleavage these two posteriorly located domains as well as those situated deeper in the egg are then split equally by the advancing furrow (Fig. 11H).

### Comparative reorganizations of zygotes in ascidians and other organisms

Actomyosin-based contractions and growth of surface microvilli at fertilization are a common feature of fertilization in several other animal species such as in amphibians (Elinson, 1983; Cheer et al., 1987), echinoderms (Terasaki, 1996) and fishes (Iwamatsu, 1998). However, in these species, microvilli

and cortical contractions do not seem to be involved in large scale reorganization and/or amplification of the preexisting egg polarity as is the case in ascidians. The situation in ascidians is probably related to a natural capping phenomenon. In fact it can be triggered by lectins which cross link surface components (Zalokar, 1980). The capping concentrates surface molecules and particles, membrane components and cortical and subcortical domains at one pole of the egg indicating that these layers are physically connected and can be considered coupled at this time.

In contrast to the initial contraction triggered by the entering sperm which sweeps through the whole egg, the repetitive constrictions in the vegetal-contraction pole that occur in the ascidian zygote during the oscillation and meiosis completion phase do not seem to be the cause of any major rearrangements of the stratified domains. These repetitive constrictions could simply reflect the response of the actomyosin network or gel to the periodic elevations of free intracellular calcium. They may be implicated in the slow (20 minutes) and progressive formation of larger and larger ER-rich cytoplasmic domains that fill the center in the zygote of ascidians and nemerteans (Speksnijder et al., 1993; Stricker et al., 1998). It is also possible that these repetitive stimulations of the cortex prime the vegetal cortex for the next event: the formation of the vegetal button. Eggs of leeches, mollusks and annelids also display cortical actomyosin-driven vegetal pole constrictions or form polar lobes at similar times in their cell cycles (Dohmen, 1983). Eggs of nematodes (*Caenorhabditis*) similarly undergo pronounced actomyosin based cortical pseudocleavage activity at this time (Hird and White, 1993).

The posterior translocation in the ascidian zygote bears some resemblance to the microtubule-dependent cortical rotation described in amphibian zygotes at about the same stage of the first mitotic cell cycle (Elinson and Palecek, 1993; Sardet et al., 1994). In *Xenopus* it has been suggested that plus end directed motors attached to the ER could provide the major force to move the vegetal cortex dorsally to a more equatorial location away from the sperm aster situated at the antipode (Houliston and Elinson, 1991; Houliston et al., 1994). Although in the much bigger egg of *Xenopus* the continuity of the translocating microtubules with those of the aster is not necessary for the displacement, it is tempting to suggest that the translocations are analogous in amphibians and ascidians and rely on the relative displacement and extension of astral microtubules and their associated cytoplasmic domains with respect to the cortex. The support for this motion (for instance the cortical ER tethered to the membrane or the membrane skeleton) as well as the molecular nature of the motors that drive these translocations remain to be characterized. It is remarkable that at this time the bulk of the cortical ER and subcortical myoplasm move posteriorly but that no movements of surface particles are detected showing that uncoupling from the surface has occurred during the phases of translocation.

We have discovered that during mitosis, there is again a brief bout of surface particle displacement. The vegetal cortex of the ascidian zygote relaxes and this apparently causes a further displacement of the bulk of the myoplasm and cortical ER domain towards the egg's equator. In a manner reminiscent of the contraction phase triggered by fertilization, the vegetal relaxation reorganization involves the cortical actomyosin network and coordinated motions of the surface and cortical and



subcortical domains. This precleavage motion is however an order of magnitude slower, and unlike the contraction triggered by fertilization, the vegetal relaxation does not seem to involve any measurable calcium signaling event (although in fishes and amphibians small calcium signals have been detected at this time; Jaffe and Creton, 1998). Precleavage waves have been observed in other eggs. They have been described in several amphibians and in the ctenophore *Beroë* (Houliston et al., 1995). They have been analyzed in some details in *Xenopus* (Hara et al., 1980; Shinagawa et al., 1989). In these large eggs, a surface relaxation and then a contraction wave are initiated in the cortex near the zygotic nucleus which is situated in the animal pole region. The waves are apparently related to the activation of mitotic kinases that propagates along the animal vegetal axis (Rankin and Kirschner, 1997; Perez-Mongiovi et al., 1998). It is possible that in ascidians, the vegetal cortex selectively responds to similar mitotic cues by a relaxation.

## II: Relocalizations and ablations of surface, cortical and cytoplasmic domains and their developmental consequences

### Surface, cortical and cytoplasmic domains

Our work on *Phallusia* clearly defines 5 domains in the vegetal region of the zygote at the end of the meiotic cell cycle. Four of these domains are organized into layers. Two of the domains clearly preexist in the egg before fertilization. These are the thin polarized layer of ER tethered to the plasma membrane (part of the isolated cortex described by Sardet et al. (1992), and the subcortical mitochondria-rich myoplasm. These two domains would be expected to contain thousands of distinct macromolecules because of their widely different composition in organelles and cytoskeletal elements. Indeed many specific proteins and RNAs have been localized in the myoplasm although for the moment none qualify as muscle determinants (reviewed by Jeffery, 1995; Satoh and Jeffery, 1995; Satoh et al., 1996; Nishida, 1997). The other domains (the surface domain consisting of a small zone rich in microvilli, the yolk-rich domain and the vegetal body) seem to form after fertilization. Two of the domains (the microvilli-rich zone and the vegetal body) appear to disperse before first cleavage. Understanding their formation, translocations, dispersion and segregation into particular blastomeres and tissues will require the identification and tracing of specific markers for these domains.

### Coupling and uncoupling of the surface, the cortex and cytoplasm

One of our conclusions is that the formation and localization of domains involves a controlled interplay between the surface and cortex of the zygote (defined as the plasma membrane and what adheres to it) and deeper cytoplasmic layers. In the ascidian *Phallusia*, the surface, cortex and the subcortical layers are tightly coupled just after fertilization (contraction phase) and just before cleavage (vegetal relaxation phase). Their coordinated motions are sensitive to Cytochalasin and probably involve the microfilamentous cytoskeleton beneath the plasma membrane. In contrast, the cortical ER and myoplasm seem uncoupled from the surface during the microtubule-driven posterior translocation phases. It will be worthwhile to examine the composition cortices isolated at different times between fertilization and cleavage (Sardet et al., 1992) and look for such coupling/uncoupling of cortex and deeper cytoplasm in different

organisms. In *Xenopus* zygotes, coupling of surface and deeper layers are manifest in the animal-directed contraction caused by fertilization that displaces the subcortical pigmented cytoplasm animally and moves the sperm and egg chromosomes closer to each other (Elinson, 1980). Then just before cleavage, surface relaxation and contraction waves preceding cleavage contribute to the aggregation of cortical islands of germ plasma and their movement towards the vegetal pole (Savage and Danilchik, 1993). This concept of coupling/uncoupling of cortical and subcortical domains with respect to the cortex may also have some relevance to the organization of the zygote of the nematode *Caenorhabditis* where initially coupled cortical and cytoplasmic (P granules) movements are followed by the independent rotation of the mitotic aster with respect to a fixed cortex (White and Strome, 1996).

### Micromanipulations, ablations and their developmental consequences

Numerous manipulations (centrifugations, delocalizations, transfers) and ablations of parts of eggs, zygotes and embryos have been performed on several species of ascidians (reviewed by Ortolani, 1958; Jeffery, 1995; Nishida, 1997). The interpretations of the results of such experiments are not straightforward for two main reasons. First, the most extensive and elegant experiments (those of Nishida that include transfers of ablated fragments) have been carried out on the large egg and zygote of *Halocynthia* whose cortical and cytoplasmic domains and their relocalizations have not been examined in great detail. Second, the effect of manipulations or ablations on the egg structure has never been thoroughly examined. It is clear that variable amounts of surface, cortex, subcortex and deeper cytoplasm are removed when cutting a fragment, but it is not known how the egg reacts to the trauma and if it recreates some of the ablated layers from surrounding regions in the way the egg plasma membrane reforms at the site of the operation (ablation) (McNeil and Steinhardt, 1997; Terasaki et al., 1997). Our experiments show that it is necessary to remove all of the contraction pole (>5% of egg volume) to alter development and that a large portion of the contraction pole proper (3% of egg volume) can be deleted without major consequences. Presumably in this case, a functional contraction pole reforms from the surrounding layers. It will now be necessary to examine the structure of the operated eggs and their functional capacity to generate repetitive calcium waves and oscillations or to carry out proper translocations.

It is tempting to superimpose the map of developmental potentialities deduced from the various ablation/fusion experiments performed on *Halocynthia*, *Phallusia*, *Styela* and *Ciona* (Fig.11 I-J-K) and the localizations of cytoplasmic domains based on our detailed observations in *Phallusia* (Fig.11A-H). A simple working hypothesis emerges from these comparisons. The fertilization-driven contraction stratifies 4 domains in the vegetal hemisphere: (1) the surface domain consisting of a zone of microvilli-rich plasma membrane, (2) the cortical ER domain, (3) the myoplasm and (4) the yolk rich domain. The bulk of domains 2 and 3 translocate in a posterior position. The bulk of the cortical ER domain is inherited by the large posterior vegetal blastomeres (B4.1) and appears progressively segregated to the smaller posterior blastomeres (B5.2, B6.3, B7.6) that arise from unequal cleavage divisions at the 16-, 32- and 64-cell stages and give rise to an endodermal

strand cell (Conklin, 1905a,b; Nishida, 1987), C. D., F. R. and C. S., unpublished data). We further suggest that this domain constitutes the precursor of the recently identified Centrosome Attracting Body (CAB) which is thought to be responsible for the unequal cleavage pattern of vegetal posterior blastomeres (Hibino et al., 1998). It is also probable that the ER-rich cortical domain is the locale for a recently identified localized maternal RNA (pem: posterior end mark; Yoshida et al., 1996). One possibility is that RNAs localized in this domain (Yoshida et al., 1997; Sasakura et al., 1998) are tethered to the ER and move with it during the first and second major phases of reorganization and then partition with the ER into the small blastomeres that arise from unequal cleavage. There is some evidence that ER is involved in the vegetal localization of RNAs in *Xenopus* oocytes (Deshler et al., 1997).

The large posterior vegetal blastomeres (B4.1 pair) of the 8-cell stage ascidian embryo that gives rise to the primary muscle cells inherit the bulk of the myoplasm and the muscle determinants that it contains. Our analysis shows also that a sizable amount (15-25%) of myoplasm is inherited by anterior vegetal blastomeres that will give rise to the secondary muscle cells as well as endoderm, notochord spinal cord and neural plate. Blastomere dissociation experiments indicate that inductive interactions may contribute to the differentiation of secondary muscle cells (reviewed by Nishida, 1997). It would be useful to analyze the partitioning of the myoplasm into the various blastomeres up to the 110-cell stage to see whether the presence of a critical mass of myoplasm is necessary for anterior blastomeres to develop into secondary muscle cells. The yolk-rich domain stratified during the contraction phase could not be followed in vivo for lack of a vital marker. If it does not move from its vegetal location it would be inherited mainly by the vegetal cells that will give rise to the endoderm cells which are known to be filled with yolk vesicles (Conklin, 1905b; Whittaker, 1977; Nishida, 1993).

The gastrulation determinants have been shown to concentrate in the vegetal pole region after the contraction phase and then spread vegetally during or after the second major phase (the translocation and vegetal relaxation phases) (Jeffery, 1992; Nishida, 1996). Since the gastrulation potential is sensitive to UV irradiation, determinants are probably localized to the most cortical layer (Jeffery, 1990a). In addition, the protein p30 lost in UV-irradiated zygotes which fail to gastrulate, is apparently linked to the cortical cytoskeleton (Jeffery, 1990b). It is likely that the gastrulation determinants are situated in the surface and cortex layer and that they are linked to the state of contractility of the vegetal pole surface and its ability to congregate (during the contraction phase) or disperse (during the vegetal relaxation phase) its microfilament-filled microvilli.

In conclusion our observations show that the ascidian zygote is organized into more stereotyped cortical and cytoplasmic domains than was previously thought and that a complex succession of events and phases participate in concentrating and positioning these domains in specific locations between fertilization and first cleavage.

We suggest that once they are localized and inherited by specific blastomeres these distinct cortical and cytoplasmic domains confer to these blastomeres the ability to undergo particular morphogenetic events (unequal cleavage/gastrulation)

or the ability to differentiate autonomously into different tissues (primary muscle/endoderm).

We are indebted to the many staff, students and colleagues who have contributed to different phases of this project in the last 7 years. Special thanks go to Annelies Speksnijder, Jean Davoust, Annie Boillot, Shinya Inoué, Philippe Dru, Brendan Flannery, Katie Auld, Caroline Huguen, Sylvain Roger, Sebastien Motreuil, and Anne Marie Gomez. We also thank Evelyn Houliston and Janet Chenevert for their comments. The work was supported by the CNRS, the MENRS (UPMC/ACCSV4) and grants from ARC and AFM to Christian Sardet.

## REFERENCES

- Bates, W. and Jeffery, W. (1987). Localization of axial determinants in the vegetal pole region of ascidian eggs. *Dev. Biol.* **124**, 65-76.
- Brownlee, C. and Dale, B. (1990). Temporal and Spatial correlation of fertilization current, calcium waves and cytoplasmic contraction in eggs of *Ciona intestinalis*. *Proc. R. Soc. Lond.* **239**, 321-328.
- Cheer, A., Vincent, J., Nuccitelli, R. and Oster, G. (1987). Cortical activity in vertebrate eggs. I: The activation waves. *J. Theor. Biol.* **124**, 377-404.
- Conklin, E. (1905a). Organ-forming substances in the eggs of ascidians. *Biol. Bull.* **8**, 205-230.
- Conklin, E. (1905b). The organization and lineage of the ascidian egg. *J. Acad. Natl. Sci. (Phila.)* **13**, 1-119.
- Conklin, E. (1931). The development of centrifuged eggs of ascidians. *J. Exp. Zool.* **60**, 1-119.
- Deshler, J., Highett, M. and Schnapp, B. (1997). Localization of *Xenopus* Vg1 mRNA by Vera protein and the endoplasmic reticulum. *Science* **276**, 1128-31.
- DiGregorio, A. and Levine, M. (1998). Ascidian embryogenesis and the origins of the chordate body plan. *Curr. opin. Gen. Dev.* **8**, 457-463.
- Dohmen, M. (1983). The polar lobe in eggs of molluscs and annelids: structure, composition, and function. In *Time, Space and Pattern in Embryonic Development* (ed. W. Jeffery and R. Raff), pp. 197-220. A.R. Liss Inc, New York.
- Eddy, E. (1975). Germ plasm and the differentiation of the germ cell line. *Int. Rev. Cytol.* **43**, 229-280.
- Elinson, R. (1980). The amphibian egg cortex in fertilization and early development. In *The Cell Surface: Mediator of Developmental Processes* (ed. S. Subtelny and N. Wessells), pp. 217-234. Academic Press, New York.
- Elinson, R. (1983). Cytoplasmic phases in the first cell cycle of the activated frog egg. *Dev. Biol.* **100**, 440-451.
- Elinson, R. and Palecek, J. (1993). Independence of two microtubule systems in fertilized frog eggs: the sperm aster and the vegetal parallel array. *Roux's Arch. Dev. Biol.* **202**, 224-232.
- Fernandez, J., Roegiers, F., Cantillana, V. and Sardet, C. (1998). Formation and localization of cytoplasmic domains in leech and ascidian zygotes. *Int. J. Dev. Biol.* **42**, 1075-1084.
- Gualtieri, R. and Sardet, C. (1989). The endoplasmic reticulum network in the ascidian egg: localization and calcium content. *Biol. Cell* **65**, 301-304.
- Hara, K., Tydeman, P. and Kirschner, M. (1980). A cytoplasmic clock with the same period as the division cycle in *Xenopus* eggs. *Proc. Natl. Acad. Sci. USA* **77**, 462-466.
- Hibino, T., Nishikata, T. and Nishida, H. (1998). Centrosome-attracting body: a novel structure closely related to unequal cleavages in the ascidian embryo. *Dev. Growth Differ.* **40**, 85-95.
- Hird, S. and White, J. (1993). Cortical and cytoplasmic flow polarity in early embryonic cells of *Caenorhabditis elegans*. *J. Cell Biol.* **121**, 1343-1355.
- Houliston, E. and Elinson, R. (1991). Patterns of microtubule polymerization relating to cortical rotation in *Xenopus laevis* eggs. *Development* **112**, 107-117.
- Houliston, E., Carre, D., Chang, P. and Sardet, C. (1995). Cytoskeleton and ctenophore development. *Curr. Top. Dev. Biol.* **31**, 41-63.
- Houliston, E., Carré, D., Johnston, J. and Sardet, C. (1993). Axis establishment and microtubule-mediated waves prior to first cleavage in *Beroë ovata*. *Development* **117**, 75-87.
- Houliston, E., Guellec, R. L., Kress, M., Philippe, M. and Guellec, K. L. (1994). The kinesin-related protein Eg5 associates with both interphase and spindle microtubules during *Xenopus* early development. *Dev. Biol.* **164**, 147-159.

- Iwamatsu, T. (1998). Studies on fertilization in the teleost. I. dynamic responses of fertilized Medaka eggs. *Develop. Growth Differ.* **40**, 475-483.
- Jaffe, L. and Creton, R. (1998). On the conservation of calcium wave speeds. *Cell Calcium* **24**, 1-8.
- Jeffery, W. (1990a). Ultraviolet irradiation during ooplasmic segregation prevents gastrulation, sensory cell induction, and axis formation in the ascidian embryo. *Dev. Biol.* **140**, 388-400.
- Jeffery, W. (1990b). An ultraviolet-sensitive maternal mRNA encoding a cytoskeletal protein may be involved in axis formation in the ascidian embryo. *Dev. Biol.* **141**, 141-148.
- Jeffery, W. (1992). A gastrulation center in the ascidian egg. *Development Supplement*, 53-63.
- Jeffery, W. (1995). Development and evolution of an egg cytoskeletal domain in ascidians. *Curr. Top. Dev. Biol.* **31**, 243-276.
- Jeffery, W. and Bates, W. (1989). Ooplasmic segregation in the ascidian *Syngaster*. In *Molecular Biology of Fertilization* (ed. H. Schatten and G. Schatten), pp. 341-367. Academic Press, New York.
- Jeffery, W. and Swalla, B. (1990). The myoplasm of ascidian eggs: a localized cytoskeletal domain with multiple roles in embryonic development. *Sem. Cell Biol.* **1**, 373-381.
- Lutz, D. and Inoue, S. (1986). Techniques for observing living gametes and embryos. *Methods in Cell Biol.* **27**, 89-110.
- McDougall, A. and Sardet, C. (1995). Function and characteristics of repetitive calcium waves associated with meiosis. *Curr. Biol.* **5**, 318-328.
- McNeil, P. and Steinhardt, R. (1997). Loss, restoration, and maintenance of plasma membrane integrity. *J. Cell Biol.* **137**, 390-393.
- Meedel, T., Crowther, R. and Whittaker, J. (1987). Determinative properties of muscle lineages in ascidian embryos. *Development* **100**, 245-260.
- Nishida, H. (1987). Cell lineage analysis in ascidian embryos by intracellular injection of a tracer enzyme III. Up to tissue restricted stage. *Dev. Biol.* **121**, 526-541.
- Nishida, H. (1992). Regionality of egg cytoplasm that promotes muscle differentiation in embryo of the ascidian, *Halocynthia roretzi*. *Development* **116**, 521-529.
- Nishida, H. (1993). Localized regions of egg cytoplasm that promote expression of endoderm-specific alkaline phosphatase in embryos of the ascidian *Halocynthia roretzi*. *Development* **118**, 1-7.
- Nishida, H. (1994). Localization of egg cytoplasm that promotes differentiation to epidermis in embryos of the ascidian, *Halocynthia roretzi*. *Development* **120**, 235-243.
- Nishida, H. (1996). Vegetal egg cytoplasm promotes gastrulation and is responsible for specification of vegetal blastomeres in embryos of the ascidian *Halocynthia roretzi*. *Development* **122**, 1271-1279.
- Nishida, H. (1997). Cell fate specification by localized cytoplasmic determinants and cell interactions in ascidian embryos. *Inter. Rev. Cytol.* **176**, 245-306.
- Nishida, H. and Satoh, N. (1985). Cell lineage analysis in ascidian embryos by intracellular injection of a tracer enzyme II. the 16 and 32 cell stages. *Dev. Biol.* **110**, 440-454.
- Ortolani, G. (1958). Cleavage and development of egg fragments in ascidians. *Acta Embryol. Morphol. Exper.* 247-272.
- Perez-Mongiovi, D., Chang, P. and Houlston, E. (1998). A propagated wave of MPF activation accompanies surface contraction waves at first mitosis in *Xenopus*. *J. Cell Sci.* **111**, 385-393.
- Rankin, S. and Kirschner, M. (1997). The surface contraction waves of *Xenopus* eggs reflect the metachronous cell-cycle state of the cytoplasm. *Curr. Biol.* **7**, 451-454.
- Reverberi, G. (1956). The mitochondrial pattern in the development of the ascidian egg. *Experientia* **12**, 55-56.
- Roegiers, F., McDougall, A. and Sardet, C. (1995). The sperm entry point defines the orientation of the calcium-induced contraction wave that directs the first phase of cytoplasmic reorganization in the ascidian egg. *Development* **121**, 3457-3466.
- Russo, G., Kozuka, K., Antonazzo, L., Tosti, E. and Dale, B. (1996). Maturation promoting factor in ascidian oocytes is regulated by different intracellular signals at meiosis I and II. *Development* **122**, 1995-2003.
- Sardet, C., McDougall, A. and Houlston, E. (1994). Cytoplasmic domains in eggs. *Trends Cell Biol.* **4**, 166-172.
- Sardet, C., Speksnijder, J., Inoue, S. and Jaffe, L. (1989). Fertilization and ooplasmic movements in the ascidian egg. *Development* **105**, 237-249.
- Sardet, C., Speksnijder, J., Terasaki, M. and Chang, P. (1992). Polarity of the ascidian egg cortex before fertilization. *Development* **115**, 221-237.
- Sasakura, Y., Ogasawara, M. and Makabe, K. (1998). *HrWnt-5*: a maternally expressed ascidian *Wnt* gene with posterior localization in early embryos. *Int. J. Dev. Biol.* **42**, 573-579.
- Satoh, N. (1994). *Developmental Biology of Ascidians*. Cambridge: Cambridge University Press.
- Satoh, N. and Jeffery, W. (1995). Chasing tails in ascidians: developmental insights into the origin and evolution of chordates. *Trends Genet.* **11**, 354-359.
- Satoh, N., Makabe, K., Katsuyama, Y., Wada, S. and Saiga, H. (1996). The ascidian embryo: An experimental system for studying genetic circuitry for embryonic cell specification and morphogenesis. *Dev. Growth Differ.* **38**, 325-340.
- Savage, R. and Danilchik, M. (1993). Dynamics of germ plasm localization and its inhibition by ultraviolet irradiation in early cleavage *Xenopus* embryos. *Dev. Biol.* **157**, 371-382.
- Sawada, T. (1988). The mechanism of ooplasmic segregation in the ascidian egg. *Zool. Sci.* **5**, 667-675.
- Sawada, T. and Schatten, G. (1988). Microtubules in ascidian eggs during meiosis, fertilization, and mitosis. *Cell Motil. Cytoskel.* **9**, 219-230.
- Sawada, T. and Schatten, G. (1989). Effects of cytoskeletal inhibitors on ooplasmic segregation and microtubule organization during fertilization and early development in the ascidian *Molgula occidentalis*. *Dev. Biol.* **132**, 331-342.
- Shinagawa, A., Konno, S., Yoshimoto, Y. and Hiramoto, Y. (1989). Nuclear involvement in localisation of the initiation site of surface contraction waves in *Xenopus* eggs. *Dev. Growth Differ.* **31**, 249-255.
- Speksnijder, J., Corson, D., Sardet, C. and Jaffe, L. (1989a). Free calcium pulses following fertilization in the ascidian egg. *Dev. Biol.* **135**, 182-190.
- Speksnijder, J., Jaffe, L. and Sardet, C. (1989b). Polarity of sperm entry in the ascidian egg. *Dev. Biol.* **133**, 180-184.
- Speksnijder, J., Sardet, C. and Jaffe, L. (1990a). The activation wave of calcium in the ascidian egg and its role in ooplasmic segregation. *J. Cell. Biol.* **110**, 1589-1598.
- Speksnijder, J., Sardet, C. and Jaffe, L. (1990b). Periodic calcium waves cross ascidian eggs after fertilization. *Dev. Biol.* **142**, 246-249.
- Speksnijder, J., Terasaki, M., Hage, W., Jaffe, L. and Sardet, C. (1993). Polarity and reorganization of the endoplasmic reticulum during fertilization and ooplasmic segregation in the ascidian egg. *J. Cell Biol.* **120**, 1337-1346.
- Stricker, S., Silva, R. and Smythe, T. (1998). Calcium and endoplasmic reticulum dynamics during oocyte maturation and fertilization in the marine worm *Cerebratulus lacteus*. *Dev. Biol.* **203**, 305-322.
- Swalla, B., Badgett, M. and Jeffery, W. (1991). Identification of a cytoskeletal protein localized in the myoplasm of ascidian eggs: localization is modified during anurid development. *Development* **111**, 425-436.
- Terasaki, M. (1996). Actin filament translocations in sea urchin eggs. *Cell Motil. Cytoskel.* **34**, 48-56.
- Terasaki, M., Miyake, K. and McNeil, P. (1997). Large plasma membrane disruptions are rapidly resealed by  $\text{Ca}^{2+}$ -dependent vesicle-vesicle fusion events. *J. Cell Biol.* **139**, 63-74.
- Venuti, J. and Jeffery, W. (1989). Cell Lineage and determination of cell fate in ascidian embryos. *Int. J. Dev. Biol.* **33**, 197-212.
- White, J. and Strome, S. (1996). Cleavage plane specification in *C. elegans*: how to divide the spoils. *Cell* **84**, 195-198.
- Whittaker, J. (1973). Segregation during ascidian embryogenesis of egg cytoplasmic information for tissue specific enzyme development. *Proc. Natl. Acad. Sci. USA* **79**, 2927-2931.
- Whittaker, J. (1977). Segregation during cleavage of a factor determining endodermal alkaline phosphatase development in ascidian embryos. *J. Exp. Zool.* **202**, 139-153.
- Yoshida, M., Sensui, N., Inoue, T., Morisawa, M. and Mikoshiba, K. (1998). Role of two series of  $\text{Ca}^{2+}$  oscillations in activation of ascidian eggs. *Dev. Biol.* **203**, 122-133.
- Yoshida, S., Marikawa, Y. and Satoh, N. (1996). *Posterior end mark*, a novel maternal gene encoding a localized factor in the ascidian embryo. *Development* **122**, 2005-2012.
- Yoshida, S., Satou, Y. and Satoh, N. (1997). Maternal genes with localized mRNA and pattern formation of the ascidian embryo. *Cold Spring Harbor Symp. Quant. Biol.* **62**, 89-96.
- Zalokar, M. (1980). Activation of ascidian eggs with lectins. *Dev. Biol.* **79**, 232-237.
- Zalokar, M. and Sardet, C. (1984). Tracing of cell lineage in embryonic development of *Phallusia mammillata* (Ascidia) by vital staining of mitochondria. *Dev. Biol.* **102**, 195-205.